Solutions to the Steady State Diffusion Equation

Introduction

In a previous set of Lecture Notes (see Ref. 1), we got our first look at the multigroup neutron balance equation. To keep things reasonably straightforward in our introductory treatment, the focus was on the diffusion theory approximation, where Fick's Law was used to approximate the net neutron current in terms of the gradient of the scalar neutron flux. After a set of formal definitions that introduced the proper multigroup notation and terminology, the resultant multigroup diffusion equation was then written using a concise matrix operator formulation, and a brief overview of the explicit operator equations used in various applications was given. The goal of Ref. 1 was to lay a solid theoretical foundation for really understanding the multigroup balance equation.

Please make sure you are comfortable with the material in Ref. 1 before continuing!!!

Now, with a good understanding of the fundamental balance equations, our emphasis will shift to the study of various analytical techniques for solution and interpretation of the resultant equations in a variety of simple, but informative, situations. This task -- the solution and interpretation of the steady state neutron balance equation -- is the real goal of this section of Lecture Notes (and the associated files that address specific example cases). In fact, the current document can be thought of as roadmap that summarizes and categorizes the many analytical examples and visualization resources that have been developed to shed some further insight into the solution of the neutron balance equation for a variety of configurations and scenarios. The various solutions addressed here (and in the associated files) are broken into two main categories -- subcritical non-multiplying systems and critical reactor systems -- with a number of sub-topics that focus on 1-group vs. 2-group systems, bare vs. reflected systems, various geometries (Cartesian, spherical, and cylindrical), etc.. In addition, a number of specific references are made concerning the nuclear data needed for performing these preliminary analyses. Thus, by the time we finish this learning module, you should be able to set up and solve the diffusion equation for a variety of configurations, obtain the nuclear data needed to quantitatively evaluate the problem solutions, and analyze and interpret the results and draw conclusions for the given problem under study.

We will first concentrate on configurations containing only moderating media (also referred to as non-multiplying systems since there is no fissionable material present), since this class of problems is relatively straightforward to solve for simple geometries. The examples treated here will give considerable insight to the behavior of neutrons in non-multiplying or mainly diffusing media. The critical reactor problem, where the fission process is the dominant source of neutrons, will then be treated once we have a good handle on some of the required mathematics needed to fully understand the behavior of such systems. The set of examples treated within both these problem classes will give us sufficient insight to do some preliminary design and analysis of real reactor systems -- such as analysis of the current UMLRR core configuration for example.

Since both problem categories rely heavily on the student's ability to obtain and interpret the solution of second order differential equations, we will start our discussions with a short review of the classification and solution of second order linear systems. However, it is mainly the

student's individual responsibility to be fairly knowledgeable in this area of mathematics (since Differential Equations is a prerequisite for this course). Thus, right now might be a good time to pick up your Differential Equations book and review the basics…

Solution of Second-Order Constant Coefficient ODEs

As a quick review of the terminology and solution methods for linear ordinary differential equations (ODEs), let's focus on the case of a 2nd order system. In particular, given the following linear 2nd order non-homogeneous (i.e. source-driven) system,

$$y''(x) + a\,y'(x) + b\,y(x) = f(x) \tag{1}$$

the ***general solution*** is given as the linear combination of the solutions to the homogeneous and particular equations,

$$y(x) = y_h(x) + y_p(x) \tag{2}$$

where $y_h(x)$ is a solution to the homogeneous (or complementary) equation

$$y''(x) + a\,y'(x) + b\,y(x) = 0 \tag{3}$$

and $y_p(x)$ is a particular solution to the original ODE given by eqn. (1). Note also that, since the highest derivative in the system is 2nd order, the general solution as given by eqn. (2) will contain two arbitrary coefficients, and a ***unique solution*** for a specific problem is obtained by satisfying two boundary conditions (which uniquely determine the two arbitrary coefficients in the general solution for source-driven systems).

The solution to a linear 2nd order constant-coefficient homogeneous ODE can be written in the form of a simple exponential, $y_h \sim e^{rx}$, where r is an unknown constant. Putting this assumed solution into eqn. (3) leads to the characteristic equation

$$r^2 + a\,r + b = 0 \tag{4}$$

Referring to r_1 and r_2 as the two distinct solutions to the characteristic equation (the case of repeated roots is a relatively uncommon occurrence), the ***homogeneous solution*** can be written as a linear combination of the individual solutions, or

$$y_h(x) = c_1 e^{r_1 x} + c_2 e^{r_2 x} \tag{5}$$

Note that for the **special case of a = 0 and b = $\pm\alpha^2$** (this is consistent with the two different forms of the 1-group diffusion equation that are commonly encountered -- see below), eqn. (3) becomes

$$y''(x) \pm \alpha^2 y(x) = 0 \tag{6}$$

which gives

$$r^2 \pm \alpha^2 = 0 \qquad \text{or} \qquad r_{1,2} = \pm\sqrt{\mp\alpha^2} \tag{7}$$

Thus, the sign of $b = \pm\alpha^2$ becomes very important, since two completely different forms for the solution can result.

When $b = -\alpha^2$, the roots are real and distinct and yield a solution written in the form of real exponentials. However, when $b = +\alpha^2$, the roots are still distinct, but now they are pure imaginary complex conjugates -- and these lead to solutions in the form of complex exponentials -- that is, the roots to the characteristic equation are $r_{1,2} = \pm i\alpha$, where i (or sometimes j) is the imaginary number $i = j = \sqrt{-1}$.

The complex exponentials are almost always written in terms of sinusoids using Euler formula,

$$e^{\pm j\alpha x} = \cos\alpha x \pm j\sin\alpha x \tag{8}$$

Thus, for the case of pure imaginary roots, eqn. (5) becomes

$$\begin{aligned} y_h(x) &= c_1 e^{j\alpha x} + c_2 e^{-j\alpha x} = c_1\left(\cos\alpha x + j\sin\alpha x\right) + c_2\left(\cos\alpha x - j\sin\alpha x\right) \\ &= \left(c_1 + c_2\right)\cos\alpha x + j\left(c_1 - c_2\right)\sin\alpha x \\ &= A_1\cos\alpha x + A_2\sin\alpha x \end{aligned} \tag{9}$$

Note that, for the case where we get real exponential solutions (for $b = -\alpha^2$), one can perform a similar manipulation using hyperbolic sinusoids. To see this, we first formally define the hyperbolic sine and cosine in terms of real exponential functions,

$$\sinh\alpha x = \frac{e^{\alpha x} - e^{-\alpha x}}{2} \qquad \text{and} \qquad \cosh\alpha x = \frac{e^{\alpha x} + e^{-\alpha x}}{2} \tag{10}$$

or $$e^{\pm\alpha x} = \cosh\alpha x \pm \sinh\alpha x \tag{11}$$

Now, for the case of real distinct roots, $r_{1,2} = \pm\alpha$, eqn. (5) becomes

$$\begin{aligned} y_h(x) &= c_1 e^{\alpha x} + c_2 e^{-\alpha x} = c_1\left(\cosh\alpha x + \sinh\alpha x\right) + c_2\left(\cosh\alpha x - \sinh\alpha x\right) \\ &= \left(c_1 + c_2\right)\cosh\alpha x + \left(c_1 - c_2\right)\sinh\alpha x \\ &= A_1\cosh\alpha x + A_2\sinh\alpha x \end{aligned} \tag{12}$$

Finally, we note that, although the first and last forms of $y_h(x)$ in eqn. (12) are equivalent, it is often more convenient to use the first form (exponential form) for infinite systems and the last form (hyperbolic sinusoids) for finite systems. This is purely a matter of convenience, but following this simple rule of thumb often minimizes the algebra needed when solving problems of this type -- and we will try to utilize this useful suggestion in the examples to follow.

In summary, the following table collects the various homogeneous solutions to the specialized ODE given in eqn. (6) -- and we will indeed use these results shortly in our subsequent examples. It should be noted, however, that the specialized solutions given here and the overall approach for obtaining these are only applicable to linear constant coefficient ODEs -- so be sure to only apply these results and techniques where appropriate!!!

$y'' - \alpha^2 y = 0$	$y'' + \alpha^2 y = 0$
$y(x) = c_1 e^{\alpha x} + c_2 e^{-\alpha x}$ (infinite region)	$y(x) = c_1 e^{j\alpha x} + c_2 e^{-j\alpha x}$ (rarely used)
$y(x) = A_1\cosh\alpha x + A_2\sinh\alpha x$ (finite region)	$y(x) = A_1\cos\alpha x + A_2\sin\alpha x$ (usual form)

Now, to complete our review, we need to say a few words about the particular solution, $y_p(x)$. There are two general techniques for finding the particular solutions to linear constant coefficient ODEs -- the Method of Undetermined Coefficients (UC method) and the Variation of Parameter Method (VOP method). The UC method is the easiest to apply, but the VOP method can be applied to a wider range of problems (see any good DE textbook for further details). Fortunately, the UC method will work just fine for all the problems we will encounter in our current study, so we will only briefly review this method within these Lecture Notes.

Within the Method of Undetermined Coefficients, one essentially makes an assumption concerning the form of $y_p(x)$, and then, via substitution of the assumed solution into the defining source-driven ODE, determines the unknown coefficients within the assumed solution. The method is relatively easy to apply once a proper form for $y_p(x)$ has been determined. This can be done by systematically applying the following two rules:

General rule: Choose $y_p(x)$ to have the same form as the RHS forcing function, f(x), ***and*** all its linearly independent derivatives. Evaluate the unknown coefficients within $y_p(x)$ by substitution into the original inhomogeneous ODE, and simply equate the coefficients of the terms with similar forms on both sides of the equation. If there are m arbitrary coefficients in the assumed $y_p(x)$ solution, this procedure will lead to m independent equations for the m unknowns. Solving these for the m coefficients gives the desired $y_p(x)$ [there should be no arbitrary coefficients in $y_p(x)$ upon completion of this procedure].

Special rule: If $y_p(x)$ via the general rule for a constant coefficient linear system contains one or more terms that are solutions to the homogeneous equation, one then multiplies these terms by x^k where k is the smallest integer value that makes all the terms in $y_p(x)$ linearly independent of the homogenous solution, $y_h(x)$ [again, you should refer to your DE text for a discussion of the Reduction of Order Method that shows where the x^k factor comes from…].

Note: As indicated above, the case of repeated roots within the homogenous solution does not occur very often in practical applications. This same statement is true when it comes to the use of the Special Rule within the UC method as noted above. However, when you took your DE course, a lot of emphasis was probably placed on these special cases since they lead to a number of interesting situations and they are certainly needed for a general treatment of the overall subject. However, in our focused treatment of the steady state neutron diffusion equation, we will not really need to apply either of these special cases…

Well, this completes our quick review of the mathematics needed to solve and interpret the diffusion equation for a number of useful situations and we will see a number of specific examples in the sections to follow. Please remember, however, that the above techniques, as illustrated here, are only applicable for linear constant-coefficient ODEs. In our work, these conditions will apply for Cartesian geometry problems with homogeneous material regions (i.e. constant material properties). However, they do not apply, in general, to spherical or cylindrical geometry situations -- and we will have to introduce other approaches for these cases. In particular, for spherical geometry problems, a simple substitution can often convert the original variable-coefficient ODE into one with constant coefficients -- and we will definitely take advantage of this simple substitution/transformation process. For cylindrical geometry problems, however, things are not so simple, and we will have to introduce a whole new class of functions (called Bessel functions) to solve problems requiring cylindrical coordinates.

In addition, we will also see that homogeneous boundary value problems can give completely different behavior relative to source driven systems -- thus, the subcritical fixed-source problem and the critical reactor problem have substantially different mathematical properties. Thus, we have a lot of mathematics to do but, in all this work, please don't lose sight of the reactor physics fundamentals we are trying to illustrate -- since this is the real goal here. The mathematics is quite interesting and quite elegant, but our real focus here is on the physical interpretations that the mathematical solutions allow us to make. Thus, in this module we will learn a lot of reactor physics as well as a lot of really neat mathematics, but the real goal here is the reactor physics insight we can glean from the various mathematical procedures that are utilized…

Non-Multiplying Source-Driven Systems

The best way to illustrate the use of the diffusion equation is to apply it to some simple, but representative, situations. We will start with the simplest of cases, and then, increase complexity as our understanding grows. In this subsection, we will restrict our analyses to cases where no fissile material is present. This restriction causes the fission source term in the general diffusion equation to vanish. In a subsequent subsection, we will concentrate on the case where fission is the dominant source term. To get started, however, it is easier to treat the simple fixed source problem first, where the source is totally independent of the neutron flux (this subject is also treated in some detail in Chapter 5 of Lamarsh -- see Ref. 2).

1-Group Problems: As a starting point, let's restrict our analyses to the 1-group approximation with no fission. This situation is appropriate when analyzing neutron attenuation in non-multiplying (diffusing) media such as reflector or shield geometries. In this case (that is, 1-group theory and no fission), the general multigroup diffusion equation (see Ref. 1) becomes

$$-\vec{\nabla}\bullet D(\vec{r})\vec{\nabla}\phi(\vec{r}) + \Sigma_a(\vec{r})\phi(\vec{r}) = Q(\vec{r}) \tag{13}$$

For a homogeneous region, the macroscopic absorption cross section and diffusion coefficient are constants. With this additional restriction, eqn. (13) becomes

$$-D\nabla^2\phi(\vec{r}) + \Sigma_a\phi(\vec{r}) = Q(\vec{r})$$

or

$$\nabla^2\phi(\vec{r}) - \frac{\Sigma_a}{D}\phi(\vec{r}) = -\frac{Q(\vec{r})}{D} \tag{14}$$

for each homogeneous region in a given problem.

Since the term containing both D and Σ_a occurs so frequently, we define the diffusion area as $L^2 = D/\Sigma_a$ and the diffusion length as $L = \sqrt{D/\Sigma_a}$. With these definitions, eqn. (14) becomes

$$\nabla^2\phi(\vec{r}) - \frac{1}{L^2}\phi(\vec{r}) = -\frac{Q(\vec{r})}{D} \tag{15}$$

Equation (15) gives the mathematical representation of neutron behavior in a 1-group, non-multiplying, homogeneous region. We will look at the solution to eqn. (15) for several standard source-geometry configurations. In particular, Table 1 summarizes the various 1-group source and geometry combinations that are treated in detail within this series of Lecture Notes, within Lamarsh (Ref. 2), and/or as potential student homework problems.

Table 1 Standard configurations that illustrate neutron diffusion using 1-group theory.

Case	Geometry Description	Source Description	Reference Material
1	infinite 1-D slab geometry	isotropic infinite planar source at x = 0	Ref. 2 and Ref. 3
2	finite 1-D slab geometry	isotropic infinite planar source at x = 0	Ref. 2 and Ref. 3
3	infinite 1-D spherical geometry	isotropic point source at r = 0	Ref. 2 and Ref. 4
4	finite 1-D spherical geometry	isotropic point source at r = 0	Ref. 4
5	two-region finite 1-D slab geometry	isotropic infinite planar source at x = 0 (at interface between two regions)	Ref. 5
6	infinite 1-D slab geometry	two isotropic infinite planar sources separated a distance H (located at x = ±H/2)	Ref. 6
7	finite 1-D slab geometry	uniformly distributed isotropic source	potential HW problem
8	two-region 1-D slab geometry (finite inner region and infinite outer region)	uniformly distributed isotropic source in inner region	potential HW problem
9	finite 1-D spherical geometry	uniformly distributed isotropic source	potential HW problem
10	two-region 1-D spherical geometry (finite inner region and infinite outer region)	uniformly distributed isotropic source in inner sphere	potential HW problem

The cases studied here include Cartesian (slab) and spherical geometry, infinite and finite region sizes, 1-region and 2-region configurations, discrete (i.e. discontinuous) and uniformly distributed sources, and even a case with multiple discrete sources. These situations cover many of the simple configurations of interest where the 1-group steady state diffusion equation can be solved analytically to get a reasonable estimate of overall behavior, and they can give the student a good understanding of neutron diffusion in typical non-multiplying systems.

Note: Most multidimensional geometries, except for a few special cases, cannot be solved analytically. Instead, they usually require numerical solution of a spatially discretized form of the balance equations (i.e. via finite difference methods). Although quite interesting, this subject is beyond the scope of this course and will not be treated here. Also, note that there are no 1-D cylindrical geometry problems in the above table of standard solutions. Although cylindrical geometry configurations are of interest here, they require the introduction of Bessel functions to solve the resultant equations. Since there is already enough mathematics associated with the above cases, we have decided to postpone our discussion of Bessel functions and the solution of cylindrical geometry problems for a bit -- until we discuss the critical reactor problem…

At this point the student should study Cases 1 - 6 in detail using the listed references. References 3 - 6, in particular, include a simple Matlab graphical user interface (GUI) that actually evaluates and plots the resultant solutions, in addition to the step-by-step mathematical treatment of the overall solution methodology. This combination -- that is, both the theory and application for a specific situation -- should give the reader a good understanding of the overall topic of neutron diffusion in a non-multiplying diffusing medium. And, with all this background, you will be well prepared to address any homework problems related to these subjects that may be assigned.

Please make sure you are comfortable with the material in Refs. 3-6 before continuing!!!

The Diffusion Length: In your analysis of Cases 1 - 6, you should have discovered the importance of the diffusion length, L, (or diffusion area, L^2) in describing the observed spatial distribution of the resultant flux profiles. To highlight this term even further, Ref. 7 shows that the diffusion length, L, is directly related to the distance traveled from birth to death of a neutron in an infinite system. In addition, Ref. 7 also shows that the simple 1-group representation and interpretation of the diffusion area and diffusion length (L^2 and L, respectively), can be easily extended to the 2-group case, where we now make a distinction between the fast and thermal diffusion properties of a given material. In particular, the fast and thermal diffusion areas, L_1^2 and L_2^2, respectively, are defined explicitly as

$$L_1^2 = \frac{D_1}{\Sigma_{a1} + \Sigma_{1\to 2}} \qquad \text{and} \qquad L_2^2 = L_T^2 = \frac{D_2}{\Sigma_{a2}} \tag{16}$$

Note also that, in a moderating medium, the primary interaction at high energy is neutron scattering. Therefore, $\Sigma_{1\to 2}$ is usually much greater than Σ_{a1} for purely moderating media. If we make this assumption, then the expression for the fast diffusion area reduces to $D_1/\Sigma_{1\to 2}$ which is typically called (for historical reasons) the thermal neutron age, τ_T, or,

$$\tau_T = \frac{D_1}{\Sigma_{1\to 2}} \tag{17}$$

The thermal neutron age (or fast diffusion area) is very similar to the thermal diffusion area, L_2^2 (or L_T^2 as used in some references -- e.g. Ref. 2), except that it applies to the fast group instead of the thermal group.

Please make sure you are comfortable with the material in Ref. 7 before continuing!!!

Cross Sections for Preliminary Calculations: In discussing the various material properties of interest, we also need to briefly address how to obtain preliminary data for both 1-group and 2-group computations involving both non-multiplying and multiplying systems. This is indeed essential so that typical problem situations can be addressed using a reasonable set of material properties for the various situations of interest. In particular, a separate set of Lecture Notes and a simple Matlab GUI (see Ref. 8) were developed to assemble, in one place, a library of data for doing computations such as these. All the data used here are based on various tabular and graphical information from Lamarsh (Ref. 2), including the equations necessary to properly account for both density and temperature variations from the tabulated reference conditions. Reference 8 details the equations and procedures used and, at this point, you should take the time

to review these Lecture Notes and associated Matlab GUI, since this information will be needed for many of the subsequent example problems and homework problems that you will encounter.

Please make sure you are comfortable with the material in Ref. 8 before continuing!!!

A 2-Group Example: Now, returning to our discussion of neutron diffusion in non-multiplying media, we should note that all the examples up to now have used 1-group theory. This was done since the mathematics is less tedious than for multigroup problems and these examples allowed us to emphasize the spatial part of the problem. In general multigroup problems, however, we have a coupled set of G 2^{nd} order differential equations which, as you might imagine, can be somewhat tedious to solve analytically. Certainly for the general case that includes fission and upscatter, this is indeed the case. However, for a non-multiplying source-driven problem with no upscatter, the G equations are only coupled in one direction -- that is, the balance equation for group g is unaffected by the neutron field at lower energies. Thus, the coupled equations can be solved sequentially starting with group 1, then group 2, etc. until the balance equations for all G groups have been evaluated.

To see this, consider the specific case of 2-group theory. For a non-multiplying medium with no upscatter, the general multigroup neutron balance equation (see Ref. 1) reduces to

$$-\vec{\nabla}\bullet D_1\vec{\nabla}\phi_1 + (\Sigma_{a1} + \Sigma_{1\to 2})\phi_1 = Q_1 \tag{18a}$$

$$-\vec{\nabla}\bullet D_2\vec{\nabla}\phi_2 + \Sigma_{a2}\phi_2 - \Sigma_{1\to 2}\phi_1 = Q_2 \tag{18b}$$

Now, if we apply these equations within a homogeneous region (with constant material properties), the leakage term simplifies considerably, allowing us to eliminate the vector notation and to divide each equation by the appropriate group diffusion coefficient. Doing this gives

$$\nabla^2\phi_1 - \frac{1}{L_1^2}\phi_1 = -\frac{Q_1}{D_1} \tag{19a}$$

$$\nabla^2\phi_2 - \frac{1}{L_2^2}\phi_2 = -\frac{Q_2}{D_2} - \frac{\Sigma_{1\to 2}}{D_2}\phi_1 \tag{19b}$$

where we have used the definitions of the fast and thermal diffusion areas from above.

Equation (19) illustrates the sequential coupling as described above. Here we see that the equation for group 1 is driven by the source Q_1, but that it is unaffected by the neutron population at lower energies (i.e. the thermal flux does not appear in the fast group balance equation). In contrast, however, the $\Sigma_{1\to 2}\phi_1$ term represents a source term for group 2 (i.e. the downscatter source), so the resultant thermal flux is clearly a direct function of the fast flux. With this overview, the scenario for solving for the flux in both groups should now be clear -- we first solve eqn. (19a) for ϕ_1 and then this can be used to develop the full source for solving for the particular and general solutions for the group 2 equation. Reference 9 illustrates this sequential solution methodology for the case of a point source of fast neutrons in an infinite moderating material. Using 2-group theory, both the fast and thermal flux profiles are derived and a short Matlab code is utilized to help visualize the spatial behavior of $\phi_1(r)$, $\phi_2(r)$, and the fast-to-thermal flux ratio, $\phi_1(r)/\phi_2(r)$, in a variety of moderator materials.

Please make sure you are comfortable with the material in Ref. 9 before continuing!!!

Well, we have now generated a variety of solutions to the diffusion equation for non-multiplying medium problems. However, before leaving this subsection, it should be cautioned that the various examples given here for neutron diffusion in moderating media were mainly illustrative of the mathematical tools needed for solving these types of problems, and for obtaining a good feeling for how the diffusion and absorption properties of a material (diffusion length or neutron age) affect the resultant flux distribution. Treating these examples from only a qualitative view is important since, in practice, the 1-group and 2-group diffusion approximations are not very accurate for finding flux distributions or dose rate predictions in shielding applications (multigroup transport theory is clearly more appropriate for this class of problems).

In contrast, however, few-group diffusion theory does give a good quantitative estimate of the neutron behavior within most critical reactor core configurations -- and this will be the subject of the next subsection. Thus, although the above methodology can only be applied in a qualitative sense for shielding analyses, the skills that we developed for analyzing the non-multiplying medium problem will be directly applicable in subsequent work, where most of our effort will be concentrated on solving and quantifying many aspects of the core physics problem (rather than shielding applications).

The Critical Reactor Problem

Much of the emphasis in this course is concerned with the detailed understanding of the behavior of neutrons within the core regions of a critical system (both research reactors and large power reactors). However, most of the topics discussed thus far are only indirectly related to core physics; they have only supplied the necessary background for a discussion of reactor core analysis. Even the last section, with its several examples illustrating the solution of the neutron diffusion equation, only emphasized applications in non-multiplying media (regions away from the core). Finally, in this section, we will discuss the critical reactor problem.

The core physics problem is somewhat unique. We know that, for steady state power production, the reactor has to be just critical. This means that there has to be a precise balance between the neutron production and loss rates. Any arbitrary mixture of fuel, moderator, and structure will not satisfy this constraint. We will find that a new restriction, usually called the ***criticality condition***, has to be satisfied. The criticality condition will interrelate the material composition and geometric configuration such that a critical system can be achieved.

These concepts will become clear as we develop the mathematics that describe the core physics problem. We will rely exclusively on the diffusion approximation to neutron transport and we will use many of the same techniques utilized in the previous section for the analysis of non-multiplying media. The primary difference in the core physics (versus shielding) problem is that now the fission source (rather than a fixed source) dominates the neutron production term. This gives rise to a subtle change in the defining equation, but it leads to a substantial change in the character of the solutions. Thus, the solution to the critical reactor problem will exhibit its own unique character.

To add some substance to this discussion, consider the general steady-state multigroup diffusion equation,

$$-\vec{\nabla}\bullet D_g(\vec{r})\vec{\nabla}\phi_g(\vec{r}) + \Sigma_{Rg}(\vec{r})\phi_g(\vec{r}) = S_g(\vec{r}) \qquad (20)$$

where the source, $S_g(\vec{r})$ is given as

$$S_g(\vec{r}) = Q_g(\vec{r}) + \chi_g \sum_{g'} \nu\Sigma_{fg'}(\vec{r})\phi_{g'}(\vec{r}) + \sum_{g'\neq g} \Sigma_{g'\to g}(\vec{r})\phi_{g'}(\vec{r}) \qquad (21)$$

This equation is general, and for any specific application, only the applicable terms are used. In most cases of interest, one of the following three situations arises:

1. Non-multiplying systems: no fission source (shielding applications)
2. Subcritical systems: both fission and external sources are important (core analyses during startup and shutdown)
3. Critical systems: no external sources (steady state core design and analysis)

The previous section focused on the case where there is no fission source. The second case must be considered in situations where both the fixed source and fission source are important. The most common situation where this arises is during reactor startup and shutdown periods. Clearly the reactor core has a substantial fission potential, but it may be arranged in a subcritical configuration (either by having some assemblies missing or by having large amounts of control inserted). Without an external source, there would be no steady state flux in this subcritical arrangement. However, in most fuel (especially fuel that has a substantial amount of burnup), there is an inherent neutron source due to the relatively large spontaneous fission and (α,n) reaction cross sections for many of the heavy actinides. The neutrons emitted from these reactions undergo subcritical multiplication (they cause fission in the fuel material) and give rise to a steady state neutron distribution throughout the system.

The analysis of subcritical systems with external (or inherent) sources utilizes the same procedures as described in the previous section. For this reason (and because of time limitations), we won't consider specific subcritical multiplication applications at this time. It is important to recognize, however, that the treatment of a subcritical fixed-source problem is only a minor generalization of the non-multiplying medium problem (so you already know how to solve problems of this type). The only consideration here is that, without the source, the system must be subcritical (leakage and absorption must dominate neutron production from fission).

To see this, consider the 1-group representation of eqns. (20) and (21) for a homogeneous subcritical configuration containing fuel, moderator, structure, and possibly some neutron poison material. For this case, the balance equation becomes

$$-D\nabla^2\phi(\vec{r}) + \Sigma_a\phi(\vec{r}) - \nu\Sigma_f\phi(\vec{r}) = Q(\vec{r})$$

or

$$\nabla^2\phi(\vec{r}) - \frac{\Sigma_a - \nu\Sigma_f}{D}\phi(\vec{r}) = -\frac{Q(\vec{r})}{D} \qquad (22)$$

Now, recall that we previously defined the neutron multiplication factor as

$$k = \frac{\text{fission neutrons in one generation}}{\text{fission neutrons in previous generation}}$$

However, all of the fission neutrons from the previous generation ultimately have to be absorbed within the reactor or leak out of the system during the current generation. Therefore, k (or k_∞ in the case of zero leakage) is given by an instantaneous balance,

$$k = \frac{\text{neutron production rate}}{\text{neutron loss rate}} = \frac{<\nu\Sigma_f\phi>}{<\Sigma_a\phi> + <-D\nabla^2\phi>} \quad \text{and} \quad k_\infty = \frac{<\nu\Sigma_f\phi>}{<\Sigma_a\phi>} = \frac{\nu\Sigma_f}{\Sigma_a} \qquad (23)$$

which says that $\Sigma_a > \nu\Sigma_f$ for a subcritical system with $k_\infty < 1$ and this leads to the conclusion that

$$\kappa^2 = \frac{\Sigma_a - \nu\Sigma_f}{D} > 0 \qquad (24)$$

Thus, for a subcritical steady-state system, eqn. (22) can be written as

$$\nabla^2\phi(\vec{r}) - \kappa^2\phi(\vec{r}) = -\frac{Q(\vec{r})}{D} \qquad (25)$$

which has the same form as eqn. (15) for a non-multiplying medium and, therefore, it is solved using identical methods.

Now, the third, and probably most important, class of problems that arise is the critical reactor problem. In this situation, the leakage and absorption rates exactly balance the neutron production from fission, and any inherent neutron source that may be present in the fuel is totally dominated by the fission source. Since the fixed source is negligible (see note below), it is simply dropped from the defining equations. Thus, eqns. (20) and (21) with $Q_g(\vec{r}) = 0$ represent a complete mathematical model of the neutron behavior in a critical reactor configuration (using the diffusion theory approximation).

For the 1-group case, the same arguments concerning the sign of the second term lead to the following expressions

$$\nabla^2\phi(\vec{r}) + \frac{\nu\Sigma_f - \Sigma_a}{D}\phi(\vec{r}) = 0$$

or $$\nabla^2\phi(\vec{r}) + B^2\phi(\vec{r}) = 0 \qquad \text{where} \qquad B^2 = \frac{\nu\Sigma_f - \Sigma_a}{D} \qquad (26)$$

In this case, B^2 is referred to as the material buckling (sometimes written as B^2_m since it is only a function of material properties), and it is written as a positive quantity since $\nu\Sigma_f \geq \Sigma_a$ in a critical system (with $k = 1$ and $k_\infty \geq 1$).

Equation (26) is the 1-group equation for a critical homogeneous reactor and we will spend a bit of time working with this expression -- since solution and analysis of this balance equation can give us a lot of insight into the core physics problem. To put this equation into perspective with our previous work, we note that the analogous representation for a homogeneous non-multiplying region was given in eqn. (15) as

$$\nabla^2\phi(\vec{r}) - \frac{1}{L^2}\phi(\vec{r}) = -\frac{Q(\vec{r})}{D} \qquad (15)$$

Note: It should be noted that if a substantial external source is inserted within a just critical reactor, the flux level starts (and continues) to increase until the source is removed. Thus, a steady-state, critical, fixed-source problem is not possible (the three terms: steady state, critical, and fixed source are contradictory). Since we are currently restricting our study to steady-state critical systems, no fixed sources will be allowed.

Besides the obvious difference on the RHS of these expressions [i.e. the lack of a fixed source in eqn. (26)], one should also note that the signs of the second term on the LHS of eqns. (26) and (15) are different -- and it is this combination of the change in sign and the fact that it is a homogeneous equation that gives rise to the fundamental differences in the character of $\varphi(\vec{r})$ for critical versus subcritical systems.

In addition, we know from the above discussion that, for a steady state critical system, there has to be a very precise balance between the neutron production and loss rates, and any arbitrary mixture of fuel, moderator, structure, and control will not satisfy this constraint. This situation is consistent with the basic nature of the defining equation for a critical reactor system -- and this occurs in many areas of physics and is referred to as a ***classical eigenvalue problem***. As detailed in Ref. 1, to emphasize this mathematical/physical form, one usually includes a mathematical eigenvalue (denoted as λ) before the fission source term in the basic defining equations.

To be explicit, let's rewrite eqn. (26) to include the eigenvalue formulation. Doing this, where we emphasize that, in a critical operating reactor, λ is unity, we have

$$\nabla^2\phi(\vec{r}) + \frac{\lambda\nu\Sigma_f - \Sigma_a}{D}\phi(\vec{r}) = 0$$

or $$\nabla^2\phi(\vec{r}) + B^2\phi(\vec{r}) = 0 \qquad \text{where} \qquad B^2 = \frac{\lambda\nu\Sigma_f - \Sigma_a}{D} \tag{27}$$

To see the significance of λ, let's integrate a slightly modified version of eqn. (27) over all space, giving

$$\left\langle -D\nabla^2\phi + \Sigma_a\phi \right\rangle - \lambda\left\langle \nu\Sigma_f\phi \right\rangle = 0$$

or

$$\lambda = \frac{\left\langle -D\nabla^2\phi + \Sigma_a\phi \right\rangle}{\left\langle \nu\Sigma_f\phi \right\rangle} = \frac{\left\langle DB^2\phi + \Sigma_a\phi \right\rangle}{\left\langle \nu\Sigma_f\phi \right\rangle} = \frac{\text{loss rate}}{\text{production rate}} \tag{28}$$

The term $\left\langle \nu\Sigma_f\phi \right\rangle$ represents the total neutron production rate from fission and $\left\langle DB^2\phi + \Sigma_a\phi \right\rangle$ represents the total loss rate (leakage + absorption). From the definition of the multiplication factor, k,

$$k = \frac{\text{production rate}}{\text{loss rate}} \tag{29}$$

we see that λ is simply the inverse of the effective multiplication factor, or

$$\lambda = \frac{1}{k} \tag{30}$$

Thus, we see that the addition of the eigenvalue within the defining equation is quite justifiable. At operating conditions, $k = 1/\lambda = 1.0$. In design analysis, however, we often want to know if a particular combination of materials will give a critical reactor. For any given material configuration, the calculated k may not be unity, but this, in fact, tells the designer how far from critical the configuration is, and that some modification is required (control in or out, more or less fuel is

required, etc.). Thus, λ is usually computed as part of the solution procedure, and it is allowed to vary from unity so that the neutron balance equation can be balanced mathematically (i.e. λ * production = loss). This approach allows considerable insight to be gained from any given reactor material distribution and geometry combination. It should be emphasized, however, that in an operating critical system, λ must be unity!!!

Now, rearranging eqns. (27) – (30) slightly gives

$$k = \frac{1}{\lambda} = \frac{\langle \nu\Sigma_f \phi \rangle}{\langle DB^2\phi + \Sigma_a\phi \rangle} \Rightarrow \frac{\nu\Sigma_f}{DB^2 + \Sigma_a} \tag{31}$$

where the last simplification assumes that the reactor can be modeled as a single homogenous region. Note also that, for an infinite system where leakage is negligible, eqn. (31) reduces to a simple expression that only includes the material properties of the system (that is, the neutron production cross section, $\nu\Sigma_f$, and the absorption cross section, Σ_a), or

$$k_\infty = \frac{\langle \nu\Sigma_f \phi \rangle}{\langle \Sigma_a \phi \rangle} \Rightarrow \frac{\nu\Sigma_f}{\Sigma_a} \tag{32}$$

Before using the above equations within some specific applications, it should be noted that the 1-group fission source can be expressed in several ways -- and varying this formulation then leads to different representations for the above equations and to alternate forms for writing k and k_∞. Thus, depending on what data may be available for a given problem, it may be convenient to alternate the choice for a given situation.

To illustrate some of the various forms, we first recall the difference between the definitions of η and ν, where

$$\eta = \frac{\text{average number of neutrons emitted}}{\text{absorption in the fuel}} \tag{33}$$

and

$$\nu = \frac{\text{average number of neutrons emitted}}{\text{fission}} \tag{34}$$

With these definitions, one can express the 1-group fission source, S_{fis}, as

$$S_{fis} = \left(\frac{\text{neutrons}}{\text{fission}}\right)\left(\frac{\text{fissions}}{\text{cm}^3 - \text{sec}}\right) = \nu\Sigma_f\phi \tag{35}$$

or $$S_{fis} = \left(\frac{\text{neutrons emitted}}{\text{absorption in fuel}}\right)\left(\frac{\text{absorptions in fuel}}{\text{cm}^3\text{-sec}}\right) = \eta\Sigma_a^F\phi \tag{36}$$

Now, we define a new term called the ***fuel utilization***, as

$$f = \text{fuel utilization} = \frac{\text{neutrons absorbed in fuel}}{\text{neutrons absorbed in complete system}} \tag{37}$$

and, for a homogeneous reactor, f can be written as

$$f = \frac{\int \Sigma_a^F(\vec{r})\phi(\vec{r})d\vec{r}}{\int \Sigma_a(\vec{r})\phi(\vec{r})d\vec{r}} = \frac{<\Sigma_a^F\phi>}{<\Sigma_a\phi>} \Rightarrow \frac{\Sigma_a^F}{\Sigma_a} \tag{38}$$

Now, using these expressions, one also has the following equivalent forms

$$S_{fis} = \nu\Sigma_f\phi = \eta\Sigma_a^F\phi = \eta f\Sigma_a\phi = k_\infty\Sigma_a\phi \tag{39}$$

where the last expression uses the 1-group k_∞ formulation from eqn. (32).

Finally, with these different representations for the fission source, we can also write the multiplication factor in various ways, as follows,

$$k = \frac{\nu\Sigma_f}{DB^2 + \Sigma_a} = \frac{\nu\Sigma_f/\Sigma_a}{L^2B^2 + 1} = \frac{k_\infty}{1 + L^2B^2} = \frac{\eta f}{1 + L^2B^2} \tag{40}$$

and we will see several applications where these various representations will be used.

One final note here, before we actually solve some problems, concerns the value of B^2 that appears in many of the above equations. If you have been paying close attention, you will have noticed that we introduced a new parameter, λ or 1/k, into the expression for B^2 in eqn. (27) and then simply solved for k in terms of B^2. These somewhat circular manipulations, of course, have introduced a new parameter, but no new equation. Thus, we cannot solve eqn. (27) for B^2 without a value for $\lambda = 1/k$, and we can't solve eqn. (40) for k without a value of B^2. Thus, we clearly need another independent constraint equation to bring closure to the above development. This closure will, of course, come naturally from the formal solution of the balance equation in eqn. (27), which we rewrite here as

$$\nabla^2\phi(\vec{r}) + B^2\phi(\vec{r}) = 0 \tag{41}$$

Equation (41) is referred to as the ***1-group critical reactor equation*** for a homogeneous region, and our job now focuses attention on the solution of this equation for a variety of simple core geometries -- and, in solving this equation, we will automatically bring closure to the dilemma concerning "***What is B^2?***"…

1-Group 1-D Problems: As we did for the non-multiplying media problem, we will start with a series of relatively simple cases, and then gradually increase complexity until we have a pretty good understanding of the overall critical reactor problem -- the goal being the solution of eqn. (41) for a variety of situations. In particular, Ref. 10 addresses this goal with a comprehensive treatment of the 1-group 1-D problem, including both bare and reflected core configurations (i.e. 1-region core and 2-region core-reflector geometries) in all three orthogonal coordinate systems (Cartesian, spherical, and cylindrical coordinates). In addition to the theoretical development, it also describes the **core_refl1g_gui** Matlab program that implements the theory within a user-friendly GUI so that the reader can easily visualize the resultant flux profiles and actually perform a series of simple design analyses for these systems. And, as you might expect, it also answers the question "***What is B^2?***"!!!

In particular, concerning B^2, Ref. 10 explains that this quantity is sometimes referred to as the **geometric buckling** and that the so-called **criticality condition** for all 1-group problems is simply that the geometric buckling, B^2_g, is identical to the material buckling, B^2_m, from eqn. (27), or

$$B^2_g = B^2_m \tag{42}$$

where, the actual value of B^2_g is determined by imposing the given boundary conditions on the problem of interest. For the 2-region core-reflector problem, the situation is the same as for the bare core problem, but its representation is a little more complex, and we see that the so-called ***critical determinant*** gives the expected criticality condition for the problem. Although the details of these different developments will not be repeated here -- since **it is expected that the reader will thoroughly study all of Ref. 10 and be familiar will all its derivations and explanations** -- we do re-emphasize that, because of a general criticality condition that will occur in every problem (some of these statements are slightly more complicated than others), the B^2 that occurs in the various expressions for the multiplication factor in eqn. (40) is indeed related to the geometric buckling (that is, the buckling that results from satisfying the physical boundary condition). Thus, eqn. (40) says that the core multiplication factor is a function of both the physical geometry (which is contained in the B^2 term) and the core material composition (D, L^2, k_∞, etc.), and this is exactly what was expected of a critical reactor system (note that, at just critical, k = 1.000).

As a summary of the solutions from Ref. 10, we reproduce Table 1 from Ref. 10 as Table 2 in the current document. This table contains a lot of information and, after a thorough review of Ref. 10, the student is expected to be familiar with all this material -- including a general understanding of the overall solution strategy as well as the detailed derivation of any of the equations listed here. Clearly the derivation of the solutions for the 2-region core-reflector cases represent more work but, even here, the solution strategy is essentially the same as for the simple bare core cases. Also, as apparent in Table 2, the cylindrical geometry configurations give solutions in terms of the ordinary and modified Bessel functions and, even though these might seem a little intimidating at first glance, they are really no more difficult to work than the well-known sinusoids and exponential functions -- once you have had a little experience with this class of functions (see Refs. 2 and 11 as well as Ref. 10 for more information about both the ordinary and modified Bessel functions).

Finally, we note that the goal of the **core_refl1g_gui** program is simply to evaluate and visualize the pertinent equations in Table 2 for each of the geometries addressed here. Thus, the student can easily get both quantitative and qualitative solutions to a variety of 1-D 1-group critical reactor problems without having to struggle with the actual implementation of the tabulated solutions -- that is, we try to make it easy here so that you can focus more of the interpretation of the physics and not have to deal with any Matlab coding or any potentially unfamiliar numerical solution techniques (such as the root finding methodology needed to get B^2 for the core-reflector cases). Thus, the combination of the theory and simple GUI implementation contained in Ref. 10 should give you all the necessary tools to fully understand the 1-group 1-D critical reactor problem -- and this is an important first step towards gaining a good overall understanding of steady-state reactor theory…

Please make sure you are comfortable with the material in Refs. 10-11 before continuing!!!

Table 2 Summary equations and various relationships for several 1-group 1-D critical systems (from Ref. 10).

Geometry	Configuration	Flux Profile	Power Normalization	Geometric Buckling
1-D Slab	**Bare Core**	$\phi(x) = A_1 \cos Bx$	$A_1 = \dfrac{PB}{2\kappa\Sigma_f \sin\dfrac{Ba_o}{2}}$	$B^2 = \left(\dfrac{\pi}{a}\right)^2$
	Core-Reflector	$\phi_c(x) = A_1 \cos Bx$ $\phi_r(x) = A_1 \cos\dfrac{Ba_o}{2} e^{-(x-a_o/2)/L_r}$		$f(B) = \cot\dfrac{Ba_o}{2} - \dfrac{L_r D_c B}{D_r} = 0$
1-D Sphere	**Bare Core**	$\phi(r) = A_2 \dfrac{\sin Br}{r}$	$A_2 = \dfrac{PB^2}{4\pi\kappa\Sigma_f \left[\sin BR_o - BR_o \cos BR_o\right]}$	$B^2 = \left(\dfrac{\pi}{R}\right)^2$
	Core-Reflector	$\phi_c(r) = A_2 \dfrac{\sin Br}{r}$ $\phi_r(r) = A_2 \sin BR_o \dfrac{e^{-(r-R_o)/L_r}}{r}$		$f(B) = D_c\left(B\cot BR_o - \dfrac{1}{R_o}\right) + D_r\left(\dfrac{1}{L_r} + \dfrac{1}{R_o}\right) = 0$
1-D Cylinder	**Bare Core**	$\phi(r) = A_1 J_0(Br)$	$A_1 = \dfrac{PB}{2\pi\kappa\Sigma_f R_o J_1(BR_o)}$	$B^2 = \left(\dfrac{2.4048}{R}\right)^2$
	Core-Reflector	$\phi_c(r) = A_1 J_0(Br)$ $\phi_r(r) = A_1 \dfrac{J_0(BR_o)}{K_0(R_o/L_r)} K_0(r/L_r)$		$f(B) = D_c B J_1(BR_o) K_0(R_o/L_r) - \dfrac{D_r}{L_r} J_0(BR_o) K_1(R_o/L_r) = 0$
Notes:	For the bare cores, the extrapolated core size is given by: $a = a_o + 2d$ or $R = R_o + d$			
	The multiplication factor for all the 1-group 1-D critical systems is given by: $k_{eff} = \dfrac{\nu\Sigma_{fc}}{D_c B^2 + \Sigma_{ac}}$			
	For the core-reflector systems, the statement $f(B) = 0$ represents a classical root finding problem, where one searches for the smallest value of B to obtain the fundamental mode solution.			

The Bare Finite Cylindrical Reactor: The previous subsection addressed several simple 1-group 1-D critical bare and reflected reactor geometries. Although it would be nice to extend this formal development to a variety of 2-D geometries, finding analytical solutions to even a simple two-region core-reflector model in 2-D geometry is not possible -- so we must resort to numerical methods to address most of the real multidimensional geometries of interest (and the subject of numerical methods is beyond the scope of this introductory treatment of reactor theory). However, one exception is the multidimensional bare homogeneous 1-region reactor problem, where an analytical technique known as the Separation of Variables method does indeed lead to an exact analytical solution for the usual Cartesian and cylindrical geometry problems.

In particular, Ref. 12 demonstrates the formal Separation of Variables solution for a bare critical homogeneous 2-D RZ cylindrical reactor. This geometry is of interest since it resembles (in a very approximate way) the core of a large PWR or BWR system (without the usual reflector region). Within this configuration, Ref. 12 shows that a cosine-shaped axial profile with a $J_0(\beta r)$ Bessel function in the radial direction is the expected form for the solution -- and it shows that we can (approximately) build the 2-D profiles in terms of the 1-D flux shapes determined previously. This is a very simplistic and approximate representation in more complicated situations, but it does allow us to visualize the general qualitative behavior of more complex systems -- which can be very useful in more realistic modeling situations. Thus, the RZ model development and visualization examples given in Ref. 12 serve to illustrate the basic ideas of the Separation of Variables solution scheme, they represent our first attempt at addressing and understanding multidimensional systems, and they give some limited insight to what might be expected in more complex 2-D and/or 3-D situations. The reader should indeed study Ref. 12 in detail to get a good handle on the overall solution methodology and to visualize the behavior of the flux and current distributions in a simple 2-D configuration.

Please make sure you are comfortable with the material in Ref. 12 before continuing!!!

2-Group Critical Systems: As noted previously, thermal reactor systems require a minimum of two energy groups to describe the actual behavior of the neutron life cycle within these systems. Up to this point we have focused only on 1-group critical systems, so now it is time to highlight the solution of the 2-group diffusion theory representation of critical systems -- and this is done in detail in Ref. 13. In particular, the formal Lecture Notes given in Ref. 13 develop a formal 2-group solution methodology for bare homogeneous systems, define the terms in the so-called 4-factor and 6-factor formulas, address how these terms can help one understand and quantify the life cycle of neutrons in a thermal system, outline how to perform preliminary critical size and composition calculations, and even address how to treat reflected systems within the context of a theory that was developed primarily for bare systems.

In general, there is a lot of fundamental reactor theory covered within this set of Lecture Notes (Ref. 13), and the student is well advised to have a good handle on this material -- since the topics covered here are key to understanding the behavior of the current generation and future generations of thermal reactors (PWRs, BWRs, HTGRs, etc.)

As a quick summary of the wealth of information available in Ref. 13, below we list several important relationships for easy reference -- however, the reader should definitely consult Ref. 13 for the detailed development and explanation of these expressions:

Formal 2-Group Theory

$$-D_1\nabla^2\phi_1 + \Sigma_{R1}\phi_1 - \lambda\left(\nu\Sigma_{f1}\phi_1 + \nu\Sigma_{f2}\phi_2\right) = 0$$

$$-D_2\nabla^2\phi_2 + \Sigma_{a2}\phi_2 - \Sigma_{1\to2}\phi_1 = 0$$

$$k_{eff} = \frac{\nu\Sigma_{f1}\left(D_2B^2 + \Sigma_{a2}\right) + \nu\Sigma_{f2}\Sigma_{1\to2}}{\left(D_1B^2 + \Sigma_{R1}\right)\left(D_2B^2 + \Sigma_{a2}\right)}$$

$$k_\infty = \frac{\nu\Sigma_{f1}\Sigma_{a2} + \nu\Sigma_{f2}\Sigma_{1\to2}}{\Sigma_{R1}\Sigma_{a2}}$$

$$\frac{\phi_1}{\phi_2} = \frac{D_2B^2 + \Sigma_{a2}}{\Sigma_{1\to2}}$$

Approximate 2-Group Theory

$$-D_1\nabla^2\phi_1 + \Sigma_{1\to2}\phi_1 - \lambda\frac{k_\infty}{p}\Sigma_{a2}\phi_2 = 0$$

$$-D_2\nabla^2\phi_2 + \Sigma_{a2}\phi_2 - p\Sigma_{1\to2}\phi_1 = 0$$

$$k_{eff} = \frac{k_\infty\Sigma_{1\to2}\Sigma_{a2}}{\left(D_1B^2 + \Sigma_{1\to2}\right)\left(D_2B^2 + \Sigma_{a2}\right)} = k_\infty P_T P_F$$

$$k_\infty = \eta_T f\, p\, \varepsilon$$

$$\frac{\phi_1}{\phi_2} = \frac{D_2B^2 + \Sigma_{a2}}{p\Sigma_{1\to2}}$$

Modified 1-Group Theory

$$k_{eff} = \frac{k_\infty}{1 + \left(L_T^2 + \tau_T\right)B^2} = \frac{k_\infty}{1 + M_T^2B^2}$$

where, in all cases,

$$\phi_1(\vec{r}) = c_1\phi(\vec{r}) \qquad \text{and} \qquad \phi_2(\vec{r}) = c_2\phi(\vec{r})$$

where $\phi(\vec{r})$ satisfies an equation of the form

$$\nabla^2\phi(\vec{r}) + B^2\phi(\vec{r}) = 0 \qquad \text{or} \qquad \nabla^2\phi(\vec{r}) = -B^2\phi(\vec{r})$$

and several of the terms in the above equations are defined as follows:

$$\text{thermal utilization} = f = \frac{\int\Sigma_{a2}^F\phi_2\,d\vec{r}}{\int\Sigma_{a2}\phi_2\,d\vec{r}} = \frac{\overline{\Sigma}_{aF}\langle\phi_2\rangle}{\left(\overline{\Sigma}_{aF} + \overline{\Sigma}_{aM}\right)\langle\phi_2\rangle} = \frac{\overline{\Sigma}_{aF}}{\overline{\Sigma}_{aF} + \overline{\Sigma}_{aM}} = \frac{\overline{\Sigma}_{aF}}{\overline{\Sigma}_a}$$

$$\text{thermal reproduction factor} = \eta_T = \frac{\int_T\eta(E)\Sigma_{aF}(E)\phi(E)\,dE}{\int_T\Sigma_{aF}(E)\phi(E)\,dE} = \frac{\langle\eta\Sigma_{aF}\phi\rangle_T}{\langle\Sigma_{aF}\phi\rangle_T}$$

$$= \frac{\langle\nu\Sigma_f\phi\rangle_T}{\langle\Sigma_a^F\phi\rangle_T} = \frac{\nu\Sigma_{f2}}{\Sigma_{a2}^F}\frac{\langle\phi_2\rangle}{\langle\phi_2\rangle} = \frac{\nu\overline{\Sigma}_f}{\overline{\Sigma}_{aF}}$$

$$\text{fast fission factor} = \varepsilon = \frac{\langle\nu\Sigma_{f1}\phi_1\rangle + \langle\nu\Sigma_{f2}\phi_2\rangle}{\langle\nu\Sigma_{f2}\phi_2\rangle} = \frac{\nu\Sigma_{f1}\langle\phi_1/\phi_2\rangle + \nu\Sigma_{f2}}{\nu\Sigma_{f2}}$$

$$\text{resonance escape probability} = p = \frac{\langle\Sigma_{1\to2}\phi_1\rangle}{\langle\Sigma_{a1}\phi_1\rangle + \langle\Sigma_{1\to2}\phi_1\rangle} = \frac{\Sigma_{1\to2}}{\Sigma_{a1} + \Sigma_{1\to2}}$$

$$\text{fast non-leakage probability} = P_F = \frac{\langle \Sigma_{1\to 2}\phi_1 \rangle}{\langle D_1 B^2 \phi_1 \rangle + \langle \Sigma_{1\to 2}\phi_1 \rangle} = \frac{1}{1+\tau_T B^2}$$

$$\text{thermal non-leakage probability} = P_T = \frac{\langle \Sigma_{a2}\phi_2 \rangle}{\langle D_2 B^2 \phi_2 \rangle + \langle \Sigma_{a2}\phi_2 \rangle} = \frac{1}{1+L_T^2 B^2}$$

$$\text{thermal migration area} = M_T = L_T^2 + \tau_T$$

Also note that a key factor in our ability to perform preliminary critical size and critical composition calculations was the assumption of a ***dilute homogeneous system***. This assumption leads to the following approximations:

$$\bar{D} \approx \frac{1}{3\bar{\Sigma}_{tr}^{M}} = \bar{D}_M \qquad \tau_T = \tau_{TM} \qquad L_T^2 = (1-f) L_{TM}^2$$

and that $p\varepsilon \approx 1.0$.

Finally, with the definition of reflector savings, δ, as the difference between the critical sizes of the bare and reflected systems, one can use the above relationships for a reflected system as well as for the bare core, where the reflected reactor uses the above equations for a bare core with an ***effective core size*** given by $a_o + 2\delta$ for a slab and $R_o + \delta$ for spherical or cylindrical geometry. Thus, the above equations can be used to do preliminary analyses for both bare and reflected 2-group critical systems -- with the formal derivations and explanations given in further detail in Ref. 13.

Please make sure you are comfortable with the material in Ref. 13 before continuing!!!

Additional Theoretical and Modeling/Analysis Considerations

The previous two sections of these notes (and the supporting reference material) cover several topics related to the solution of the steady state diffusion equation for both source driven and critical reactor systems. Although this material gives a good introductory overview of steady-state reactor theory, it certainly does not represent a complete treatise on this subject -- and there are many important topics that have not been discussed and/or only an elementary treatment has been given here. Much of the omitted material is clearly not appropriate for discussion in an introductory course (transport theory solutions, numerical solution of the balance equations, etc.), but some subjects have not been discussed in detail simply due to a lack of time. However, in an attempt to be as complete as possible, we will briefly mention a few of the missing topics here, just so you are at least vaguely familiar with some of the considerations that have been neglected in previous discussions. In addition, the simple geometries treated previous have given us a good idea of the expected flux behavior in a variety of situations, but there are also many cases that have not been addressed. Thus, we will show some real modeling and analysis results for a simple 2-group 2-D core-reflector model and for a typical core configuration within the UMass-Lowell research reactor (UMLRR), just so we can point out some interesting situations that cannot be treated easily with simple analytical models.

In particular, we want to briefly address four additional topics, as identified in the following subsections:

Heterogeneous Effects: We have consistently used the term "homogeneous" to describe the material properties in all our previous models. Clearly, however, reactor geometries are not simple homogeneous mixtures of fuel, moderator/coolant, structure, and control. Instead, the actual geometries are quite complicated and quite heterogeneous -- with discrete regions of fuel, clad, coolant, structure, etc.. Figures 1 and 2 highlight this heterogeneous geometry, with a detailed sketch of a typical Westinghouse PWR 17×17 fuel assembly and a simple drawing of the core region for the UMLRR -- clearly these geometries are not physically homogeneous!!!

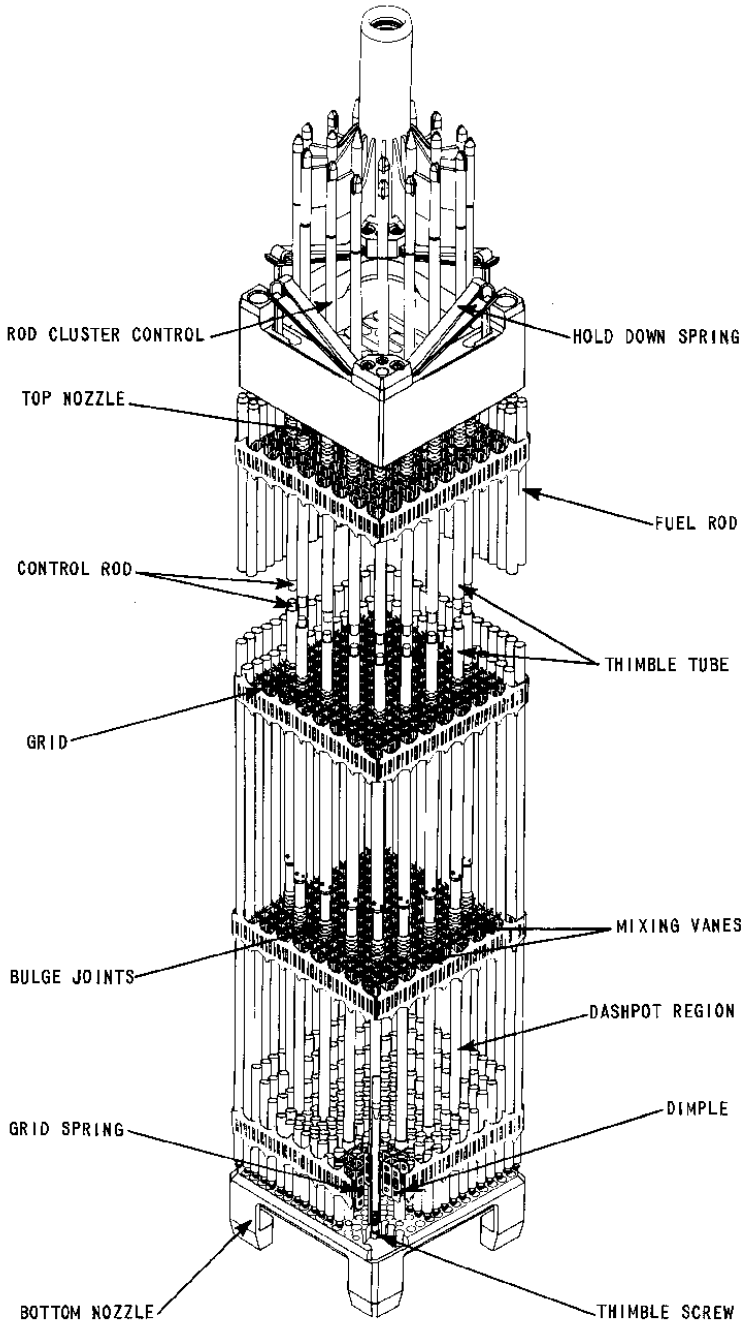

Fig. 1 Standard Westinghouse PWR 17×17 fuel assembly design.

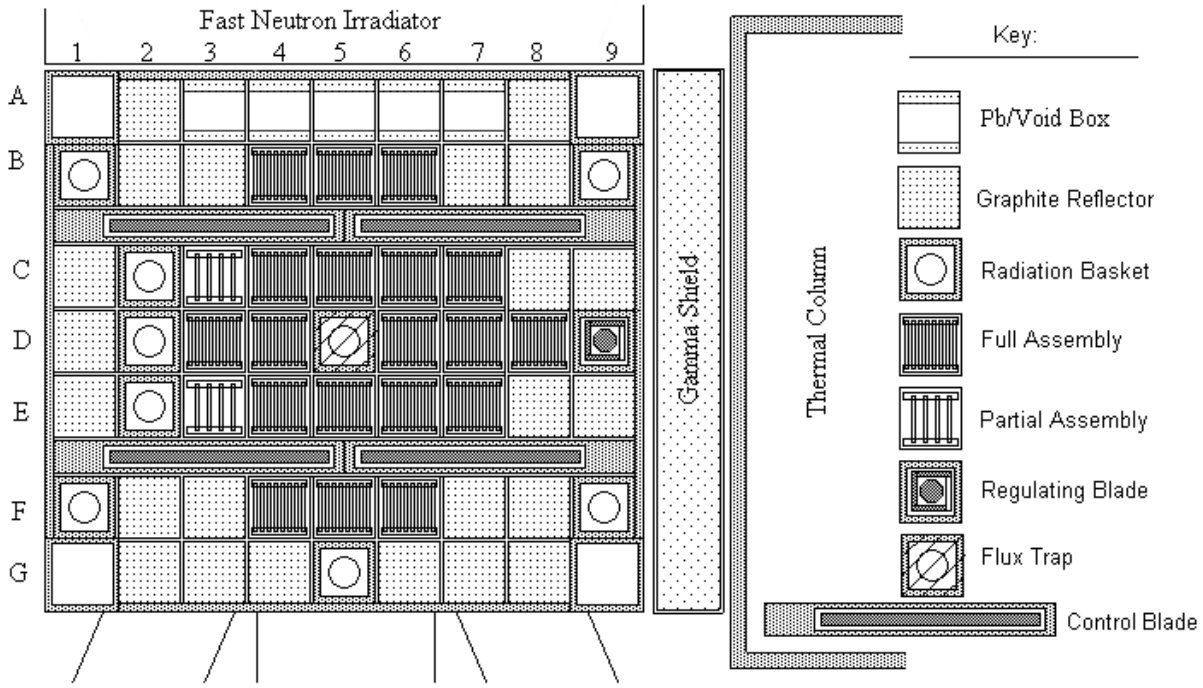

Fig. 2 Post-FNI core layout within the UMLRR.

The challenge then becomes "How do we create equivalent homogeneous regions that properly account for the heterogeneous detail in the physically heterogeneous geometries?". This task is usually treated as part of the cross section averaging and collapsing process as discussed briefly in a previous set of Lecture Notes (see Ref. 14). In general, this process is quite involved and a few paragraphs excerpted from Ref. 14 overviews the key issues involved, as follows:

---------- excerpt from Ref. 14 with minor editing ----------

The equation to be used for collapsing the fine group data for some spatial region z is of the form

$$\sigma_{gz} = \frac{\frac{1}{N_z}\sum_{g'\in g}\int_{v_z} N(\vec{r})\sigma_{g'}(\vec{r})\phi_{g'}(\vec{r})d\vec{r}}{\sum_{g'\in g}\int_{v_z}\phi_{g'}(\vec{r})d\vec{r}}$$

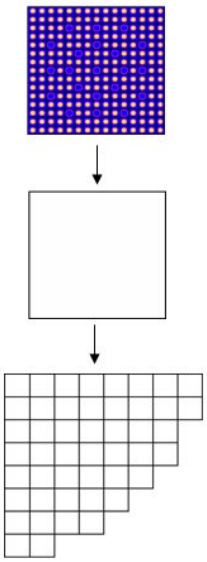

where g' refers to the fine group number and g is a broad group index. To evaluate this equation, one needs to know the geometry (denoted by the spatial variable $\vec{r}$ and domain of interest v_z), the material composition (denoted by $N(\vec{r})$ and its average value over v_z as N_z), and the spatial variation of the fine group weight function, $\phi_{g'}(\vec{r})$. This typically requires that a fine group 1-D or 2-D model be employed to solve for $\phi_{g'}(\vec{r})$.

In doing this, some representative portion of the overall heterogeneous geometry is modeled in one-dimensional or two-dimensional geometry. This unit cell or unit assembly calculation is designed to be simple enough so that $\phi_{g'}(\vec{r})$ can be computed, but accurate enough so that the resultant

average cross sections are indicative of a full multidimensional heterogeneous geometry fine group analysis. The broad group cell or assembly averaged cross sections can then be used in full or partial core 2-D and 3-D computer models that only incorporate homogeneous regions within the models.

The key goal, of course, is to somehow incorporate all the detailed information that is available in the heterogeneous geometry and fine-group energy resolution into the broad group assembly averaged cross sections. This is not an easy task, and there is still ongoing research on how best to accomplish this task. The two key issues involved here relate to the concepts of space and energy self shielding. These two concepts are illustrated nicely in the two sketches: one showing the flux depression that can occur in the neighborhood of a resonance, and the other showing the depression in the thermal flux that often occurs in the vicinity of a fuel rod (or other absorber material). These indicate the fine detail that must be accounted for in the space and energy dependent weight function, $\phi_{g'}(\vec{r})$, when collapsing to the problem-dependent broad group level.

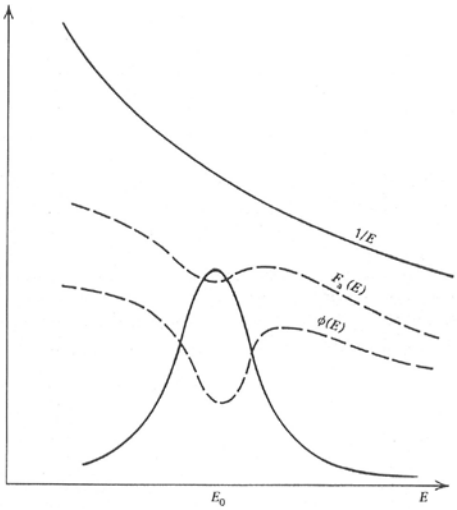

Flux depression in the neighborhood of a resonance.

Clearly some details have been left out of the above discussion. In addition, it should be noted that there is no single path to follow, and it is somewhat of an art to perform these kinds of computations. The definition of the unit cell, the choice of the initial fine group and resultant broad group energy structures, and the selection of the calculational methods to compute $\phi_{g'}(\vec{r})$ are decisions that need to be made. Only some experience (and good fortune) will get you through the torturous path of generating broad group cross sections.

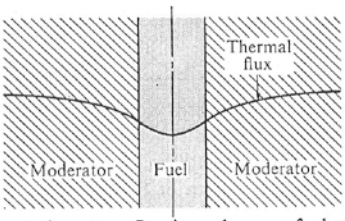

Thermal neutron flux in and near a fuel rod.

Lamarsh (Ref. 2) also addresses the subject of heterogeneous systems, with focus on how the components of the 4-factor formula change for heterogeneous versus homogenous systems. This discussion is instructive from a qualitative viewpoint, but sophisticated computer modeling, as noted above, is usually needed for quantitative results. The two factors mostly affected are the thermal utilization, f, and the resonance escape probability, p. Within this context, lumping of the fuel tends to reduce the thermal flux in the fuel region (spatial self shielding) and this tends to decrease the thermal absorption rate in the fuel -- thus $f_{het} < f_{homo}$. Concerning the resonance region, lumping of the fuel also increases the atom density and macroscopic absorption cross sections in these resonances. This, in turn, can cause a flux dip at the localized resonance energies (resonance self shielding) and this tends to decrease resonance absorption and increase the resonance escape probability -- thus $p_{het} > p_{homo}$. In most low enriched systems, since the average absorption cross section at resonance energies is greater than at thermal, the lumping of the fuel generally increases p more than it decreases f. Thus, $(pf)_{het} > (pf)_{homo}$ for low enriched systems. However, it should be noted that these effects are quite subtle, and detailed computer modeling is usually needed to quantify these effects for design and analysis purposes.

Coupling of Thermal Hydraulics and Reactor Physics: Before any reactor physics computations can occur, we must have knowledge of the material composition and temperature, so that the appropriate atom densities and macroscopic cross sections can be determined. However, in practice, the computed flux distribution and power density profile affect the material temperature and density distribution which, in turn, impacts the physics calculation, etc. etc. This coupling represents a nonlinear relationship, since the cross sections are implicitly related to the computed flux and power distribution. In addition, since the temperatures and densities are spatially dependent, the macroscopic cross sections are also functions of space (fuel burnup also causes a spatial dependence). This spatial behavior and nonlinear coupling is definitely important in high power systems, and this is usually treated within a nonlinear iteration scheme within the design codes used within the nuclear industry.

The energy removal process will be discussed in some detail and some actual heat transfer calculations will be performed in your subsequent Reactor Engineering course that will allow you to estimate the fuel and coolant temperature profiles in an operating PWR and BWR. However, at this point, it is sufficient to note that the connection between the physics calculations and the thermal-hydraulic computations is the power density, PD, where

$$PD(\vec{r}) = \kappa \sum_g \Sigma_{fg}(\vec{r})\phi_g(\vec{r}) \tag{43}$$

Note also that, in the heat transfer literature, the internal heat generation term is often given as q''' -- so, in nuclear heat transport studies, $q'''(\vec{r}) = PD(\vec{r})$ for the configuration under study (with usual units of W/cm^3 or BTU/ft^3). Thus, the physics calculation feeds the thermal-hydraulic analysis and, in turn, the resultant temperature profile allows us to compute the appropriate macroscopic cross sections for the system -- and this nonlinear iteration scheme is continued until the power density and temperature profiles no longer change…

Within this context, it should also be noted that the physics analysis also feeds any safety calculations that will be performed for a given reactor system. In safety analyses, one is often interested in the worst case scenario, so usually the hottest assembly and/or hottest channel is the focus of the analysis. For a hot channel analysis, we are interested in the fuel pin and channel configuration with the maximum power production, since this often leads to the highest temperatures and the greatest potential for fuel damage -- and excessive temperatures that can lead to fuel damage must be avoided under all plausible accident scenarios.

The power peaking factor, F, and/or the hot channel factor, F_R, are the usual quantities that are passed along from the physics analysis team to the safety analysis group. The total peaking factor is simply a ratio of the peak to average power density, or

$$F = \frac{PD_{max}}{PD_{ave}} \tag{44}$$

where the power density at a point is given by eqn. (43), and the hot channel factor (which is sometimes referred to as the radial peaking factor) is given by

$$F_R = \frac{\text{maximum pin power}}{\text{average pin power}} \tag{45}$$

These two quantities are clearly related by the axial peaking factor, F_z, which represents the peak to average power density along the hot fuel pin. In particular, we have

$$F = F_R F_z \tag{46}$$

These peaking factors are important because, with these quantities, one can easily construct the peak heat generation rates within the hot channel, or

$$\text{max power density} = F \times PD_{ave} = F\left(\frac{P}{V_{fuel}}\right) \tag{47}$$

$$\begin{matrix}\text{power produced} \\ \text{in hot pin}\end{matrix} = F_R \times \text{ave pin power} = F_R\left(\frac{P}{\#\text{ of fuel pins}}\right) \tag{48}$$

where P is the total reactor power and V_{fuel} is the total volume of all the fuel pins. Since the average power density and the average pin power are readily available quantities, if F and F_R are known, then eqns. (47) and (48) can be easily evaluated for these two important quantities -- that is, the maximum power density in the system and the power (or average power density) produced in the hottest fuel pin in the reactor.

In general, F, F_R, and F_z are determined from detailed physics calculations for the system under study -- and this is usually done via numerical solution of the multigroup neutron balance equation and appropriate manipulation of the resultant discrete power density distribution. However, if the core geometry is simple enough to allow analytical calculations, then these quantities can be determined from simple integration of the analytical results.

As an example, let's consider the finite bare homogeneous cylindrical reactor model from Ref. 12. In this 1-group case, the resultant power density is given by

$$PD(r,z) = \kappa\Sigma_f\phi(r,z) \tag{49}$$

and the total reactor power is simply the integral of eqn. (49) over the full core volume, or

$$P = \int \kappa\Sigma_f\phi d\vec{r} = \kappa\Sigma_f \int \phi(r,z)\,2\pi r dr dz \tag{50}$$

where κ is an energy per fission conversion factor (200 MeV/fission = 3.204×10-11 W-s/fission) and

$$\phi(r,z) = AJ_0\left(\frac{2.4048}{R}r\right)\cos\left(\frac{\pi}{H}z\right) \tag{51}$$

Since this is a bare homogeneous system, the maximum power density clearly occurs at the center of the reactor (at r = 0 and z = 0), so that PD_{max} is simply

$$PD_{max} = \kappa\Sigma_f A = \kappa\Sigma_f\left(\frac{2.4048\pi}{4J_1(2.4048)}\frac{P}{\kappa\Sigma_f V_{fuel}}\right) = \frac{3.638P}{V_{fuel}} \tag{51}$$

where the expression for A comes directly from Ref. 12 and assumes that the extrapolation distances are small (i.e. $H \approx H_o$ and $R \approx R_o$).

Now, since the total peaking factor is simply a ratio of the peak to average power density, we have

$$F = \frac{PD_{max}}{PD_{ave}} = \frac{\dfrac{3.638P}{V_{fuel}}}{\dfrac{P}{V_{fuel}}} = 3.638 \tag{52}$$

Also, since the peak in the axial profile occurs at z = 0, the radial power density profile at this axial location is given by

$$PD(r,0) = \kappa\Sigma_f \phi(r,z)\big|_{z=0} = \kappa\Sigma_f A J_0\left(\frac{2.4048}{R} r\right) = c_1 J_0\left(\frac{2.4048}{R} r\right) \tag{53}$$

and the radial peaking factor is given by

$$\begin{aligned} F_R &= \frac{PD(r,0)\big|_{max}}{PD(r,0)\big|_{ave}} = \frac{c_1}{\dfrac{2\pi c_1}{\pi R_o^2}\displaystyle\int_0^{R_o} r\, J_0\left(\frac{2.4048 r}{R}\right) dr} \\ &= \frac{c_1}{\dfrac{2\pi c_1}{\pi R_o^2}\dfrac{R_o R}{2.4048} J_1\left(\dfrac{2.4048 R_o}{R}\right)} \approx \frac{2.4048}{2J_1(2.4048)} = 2.316 \end{aligned} \tag{54}$$

where again, the final evaluation assumes that the extrapolation distance is small, and the result for the integration over the core volume comes directly from Ref. 12.

Doing the same type of analysis for the axial peaking factor at r = 0, gives

$$PD(0,z) = \kappa\Sigma_f \phi(r,z)\big|_{r=0} = \kappa\Sigma_f A \cos\left(\frac{\pi}{H} z\right) = c_2 \cos\left(\frac{\pi}{H} z\right) \tag{55}$$

and

$$F_z = \frac{PD(0,z)\big|_{max}}{PD(0,z)\big|_{ave}} = \frac{c_2}{\dfrac{c_2}{H_o}\displaystyle\int_{-H_o/2}^{H_o/2} \cos\frac{\pi z}{H} dz} = \frac{c_2}{\dfrac{c_2}{H_o}\dfrac{2H}{\pi}\sin\dfrac{\pi H_o}{2H}} \approx \frac{\pi}{2} = 1.571 \tag{56}$$

where we note that these results are indeed consistent with eqn. (46), since

$$F = F_R F_z = (2.316)(1.571) = 3.638 \tag{57}$$

The various peaking factors defined here are extremely important in reactor design and safety analysis studies, and these will be addressed again in some detail in your subsequent Reactor Engineering class. For now, we emphasize that computing these quantities is one of the primary goals (among several others) of the reactor physics analysis, and they represent the primary link between the reactor physics and thermal hydraulics groups within many nuclear design and analysis organizations.

A Simple 2-D Core-Reflector Model using 2-Group Theory: The sequence of examples illustrated previously were, out of necessity, quite simple -- since we needed to confine the problem specifications to meet several criteria so that the resultant differential equations would indeed be solvable using relatively straightforward analytical methods (homogeneous material compositions, one or two regions, 1 or 2 energy groups, various 1-D geometries, bare

homogeneous 2-D geometries, etc.). In practice, of course, real reactor systems are much more complicated than implied by these simple configurations, but most of the more realistic models cannot be addressed using analytical methods. In this subsection we illustrate, using the VENTURE code[15], the flux distribution that results for a relatively simple 2-group reflected reactor modeled in 2-D XY geometry (this system cannot be solved analytically). The VENTURE code solves 1-D, 2-D, and 3-D reactor geometries using the multigroup diffusion theory representation of the neutron balance equation -- and it is relatively easy to use for simple geometries if appropriate cross sections are available.

For the demo here, we use a well-known PWR benchmark model[16] that was used extensively in the 1980s and early 1990s to validate a lot of the computational methods development that was being done at that time. Most of the so-called IAEA PWR Benchmark specifications are summarized nicely in Fig. 3. Enough details are available here to model the full 1/8-core symmetric 3-D system but, for illustration here, we only address the 2-D XY planar region at the axial centerline of the system. In addition, we have taken the liberty to modify the formal benchmark and include a model without control as well as the reference 2-D mid-core model with control inserted within four assemblies as implied in Fig. 3.

The two 2-D models used here are illustrated in Fig. 4, where the top configuration shows the model with no control inserted (i.e. a simple core-reflector system), and the bottom layout shows the reference benchmark configuration with control in four assemblies within the ¼ core model. VENTURE models, using the 2-group data given on the specification sheet, were developed and run, and the output flux files were post-processed with a series of in-house Matlab codes to generate various views of the resultant flux distributions within the two models. These profiles are summarized in Figs. 5–10, as follows:

Figure 5 shows the X-directed group-dependent flux profiles for the control-out and control-in cases near the centerline of the core (through $y \approx 169$ cm). In particular, both figures clearly show a peak in the thermal flux just beyond the core-reflector interface. This buildup of thermal neutrons is primarily due to the discontinuous material properties at the interface, where the reflector thermal absorption cross section is significantly lower than in the core region (about a factor of 8 for the current system). Thus, the fast fission neutrons slowing down in this region tend to increase the thermal neutron flux (because of the reduced absorption relative to the core region) and produce a very distinctive peak in the thermal flux profile. This thermal peaking is an important effect and it certainly must be modeled accurately in thermal systems -- and this is one reason why 1-group theory is not really appropriate for thermal reactor systems.

For the control versus no control cases, we clearly see that, in the vicinity of the poisoned assemblies, there are significant depressions in both the fast and thermal flux profiles. Here the larger thermal absorption cross section causes a reduction in the thermal flux and, in turn, the lower thermal flux reduces the fission rate near these assemblies, which causes the depression in the fast flux. The y location for the profiles in Fig. 5 goes directly through the center of the rodded assemblies but, in Fig. 6, the y location for the selected profiles (at $y \approx 150$ cm) does not pass directly through any controlled assemblies. However, even in this location, the effect of the nearby control rods is still apparent -- although the flux depressions are significantly reduced.

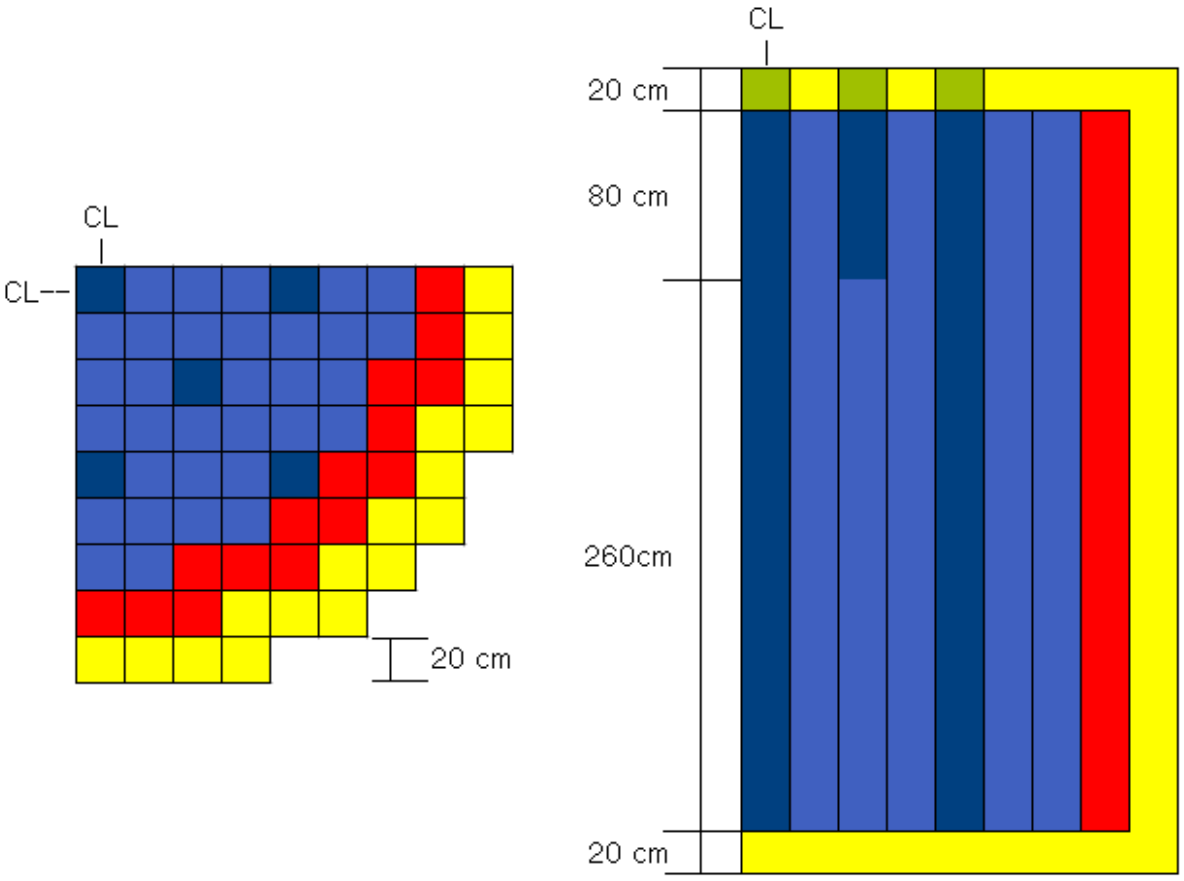

Core Geometry

Two Group Cross Sections for Each Composition

Material		D_g	Σ_{ag}	$\nu\Sigma_{fg}$	$\Sigma_{s2<-1}$
	Fuel1	1.500	0.010	0.000	0.020
		0.400	0.085	0.135	
	Fuel1+Rod	1.500	0.010	0.000	0.020
		0.400	0.130	0.135	
	Fuel2	1.500	0.010	0.000	0.020
		0.400	0.080	0.135	
	Reflector	2.000	0.000	0.000	0.040
		0.300	0.010	0.000	
	Reflector+Rod	2.000	0.000	0.000	0.040
		0.300	0.055	0.000	

Fig. 3 Specifications for the 2-D/3-D IAEA PWR Benchmark (from Ref. 16).

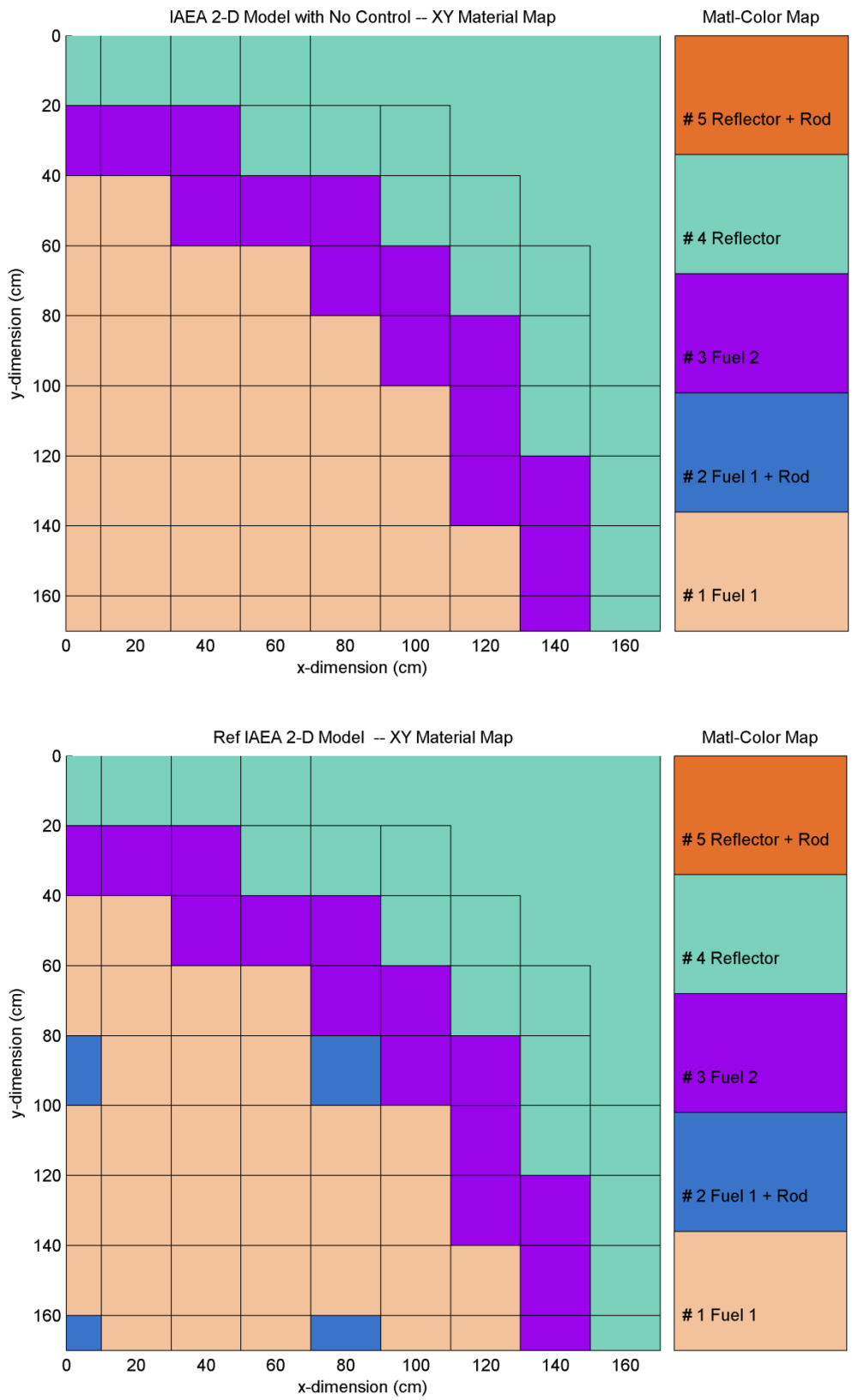

Fig. 4 Material layouts for the two 2-D cases treated here (without & with control).

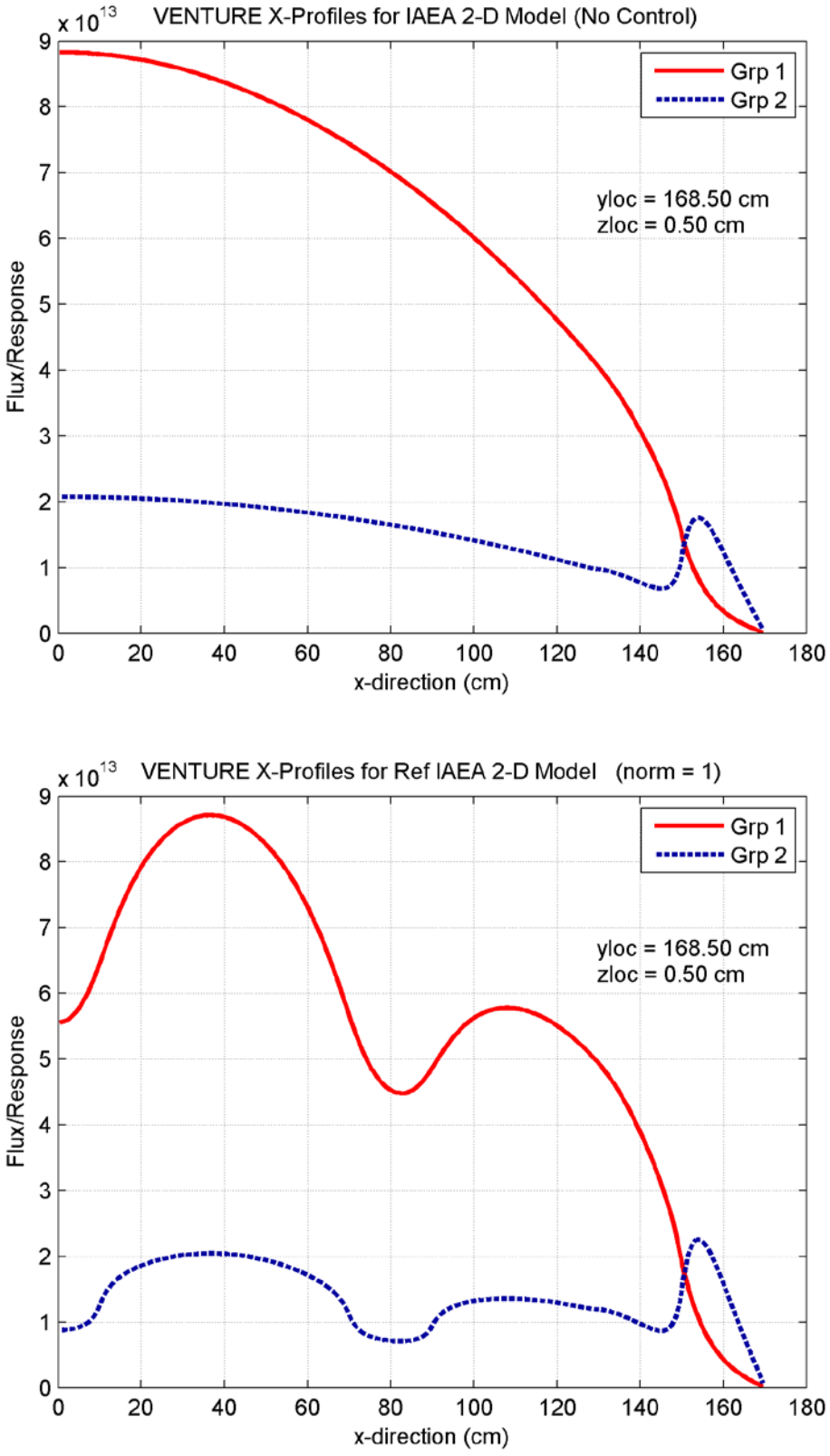

Fig. 5 X-directed flux profiles at y ≈ 169 cm.

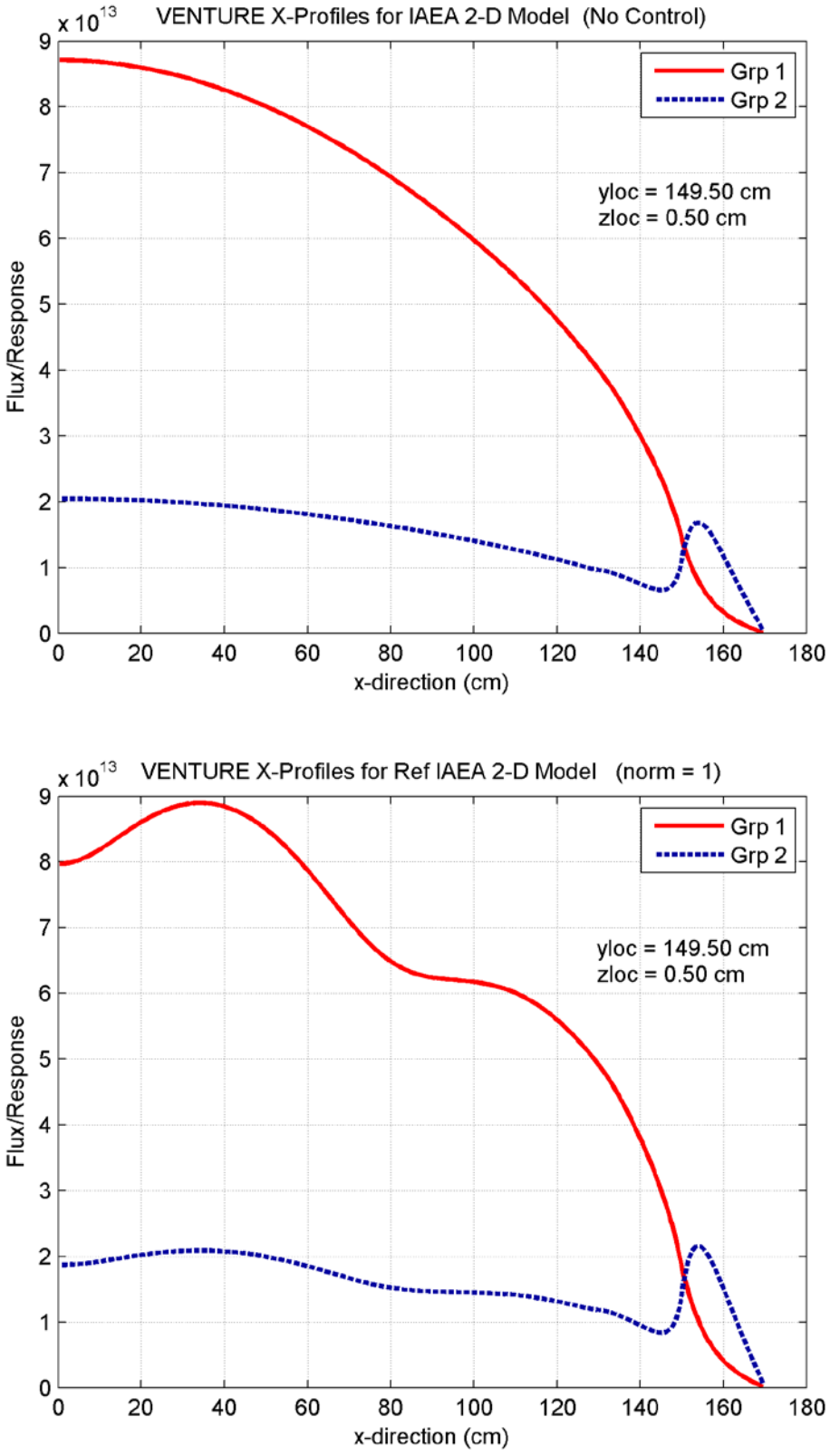

Fig. 6 X-directed flux profiles at y ≈ 150 cm.

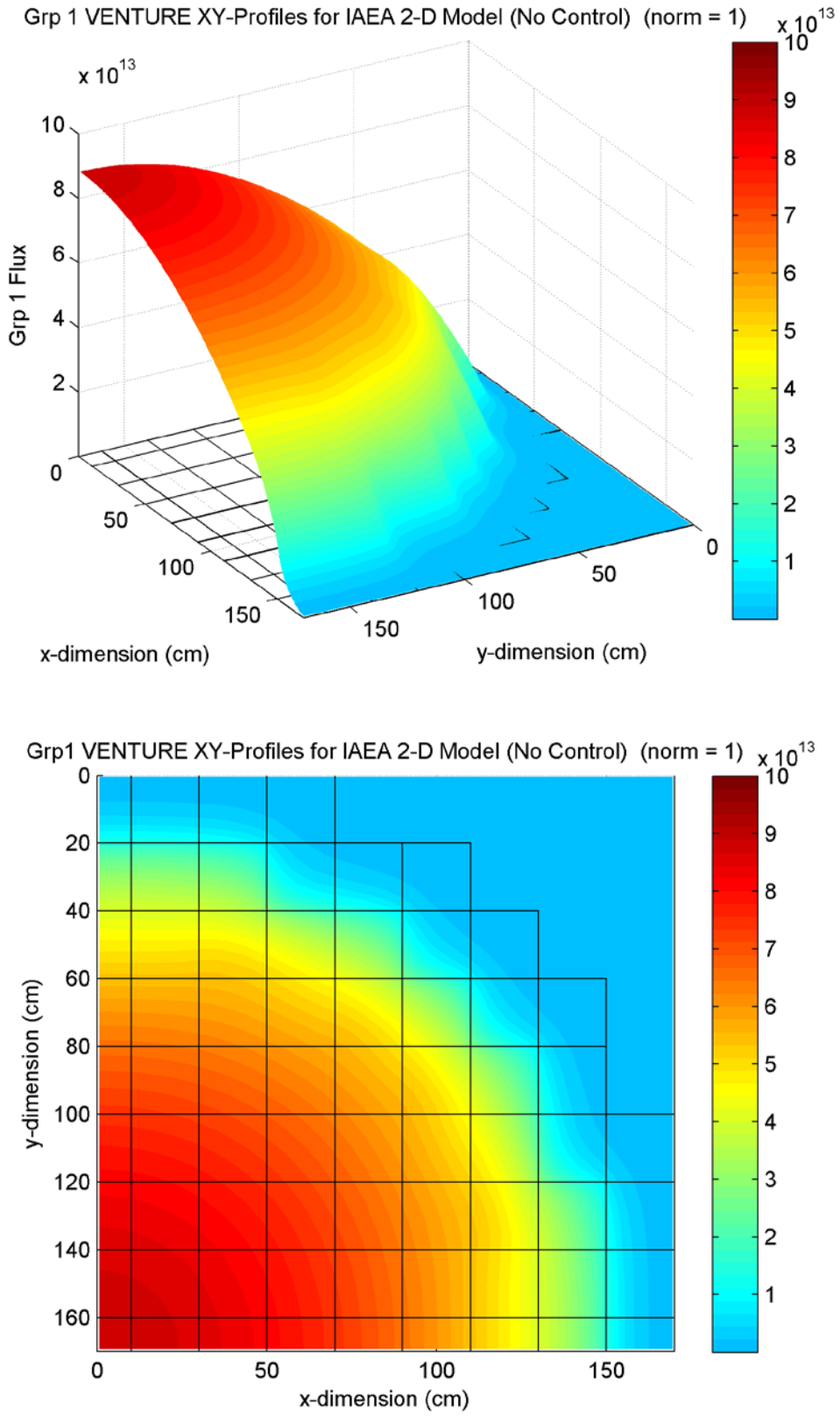

Fig. 7 Isometric and top view of the fast flux distribution for the case with no control.

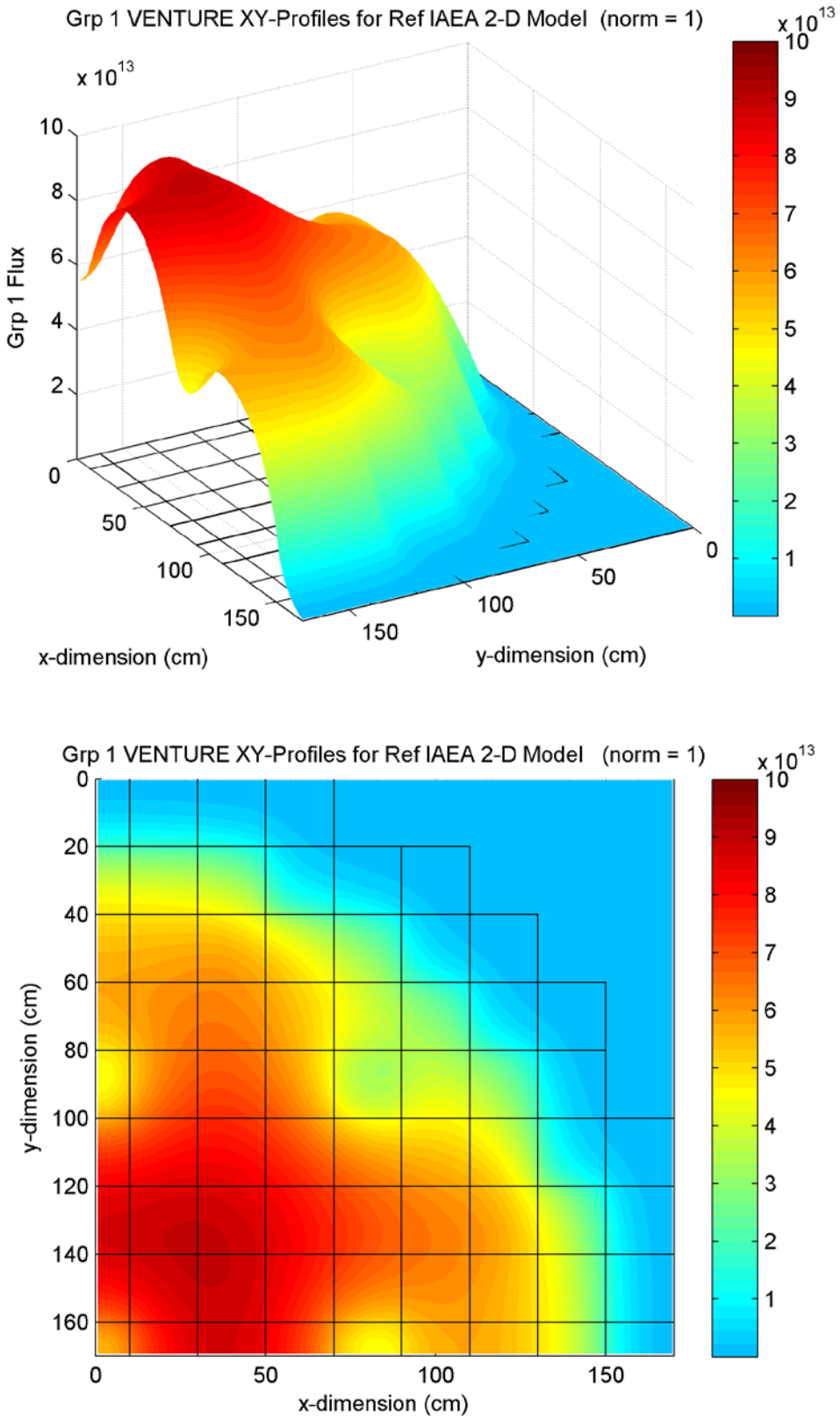

Fig. 8 Isometric and top view of the fast flux distribution for the case with control.

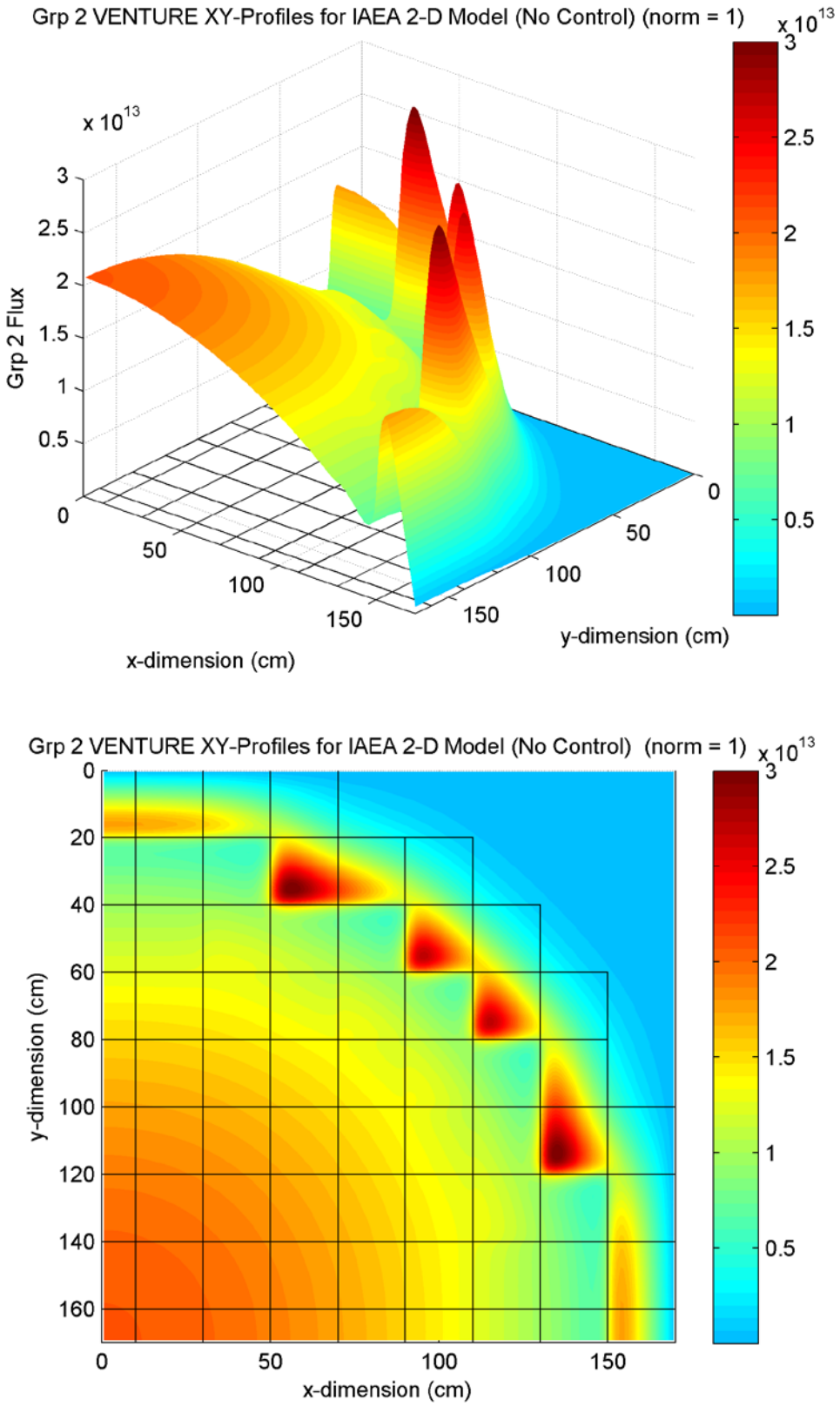

Fig. 9 Isometric and top view of the thermal flux distribution for the case with no control.

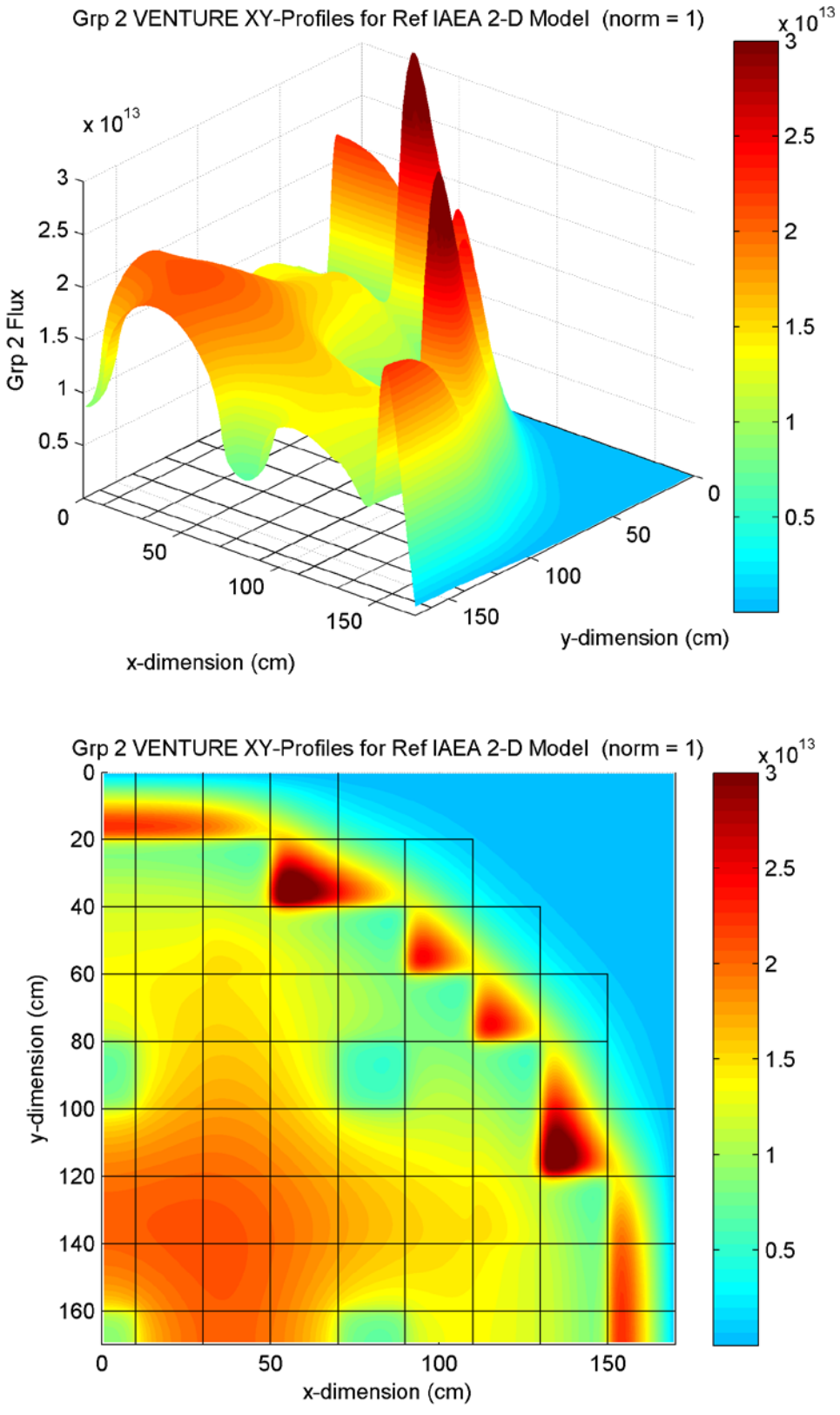

Fig. 10 Isometric and top view of the thermal flux distribution for the case with control.

Figures 5 and 6 give a quantitative view of the two primary effects of interest here -- the flux depression due to the control rods within certain assemblies and the peak in the thermal flux that usually occurs at the core-reflector interface in a thermal reactor. For a more qualitative view, Figs. 7-10 show the fast and thermal surface plots (isometric and top views) for both the no control and controlled cases. These allow a better overall perspective of the expected flux distribution throughout the full configuration in these relatively simple systems. The various peaks and valleys in the flux profiles shown here are typical, and these same features are observed in more complex systems each time there are large changes in macroscopic cross sections across material boundaries within the overall system.

Some Analyses for the UMLRR: Here we use the UMass-Lowell research reactor (UMLRR) to illustrate the behavior of actual flux profiles within a real reactor system. As indicated previously, the UMLRR was converted from the use of high enriched uranium (HEU) fuel to low enriched uranium fuel (LEU) in August 2000 and a new large-volume fast neutron irradiation (FNI) facility was designed and installed within the UMLRR in early 2002. To support these design efforts, a series of computational models within the VENTURE[15] and DORT[17] codes were developed and used to design the new configurations and to help analyze the actual as-built systems. VENTURE uses diffusion theory and allows 1-D, 2-D, or 3-D modeling, and DORT uses the transport theory approximation which allows treatment of the angular dependence of the neutron flux in 2-D configurations. The VENTURE models typically use two energy groups, where the focus is on computing the multiplication factor, blade worth distributions, and other reactivity-related parameters, as well as determining the overall power distribution in the system. For the 2-D DORT analyses, we typically use a coupled 47-group neutron and 20-group gamma cross section library so that we can get detailed representations of both the multigroup neutron and gamma radiation fields throughout the facility -- with special focus on characterization of the experimental facilities within the UMLRR.

Several papers (see Refs. 18-25) have been written over the years for both internal use at UMass-Lowell and for presentation at a number of national and international conferences that summarize the UMass-Lowell design and analysis work for the HEU to LEU conversion effort and for the development and initial testing of the FNI facility. Clearly, we do not have the time to go over all this work in detail -- but you are certainly encouraged to review the appropriate references in more detail if you have interest. Instead, as part of these Lectures Notes, we simply show a series of selected diagrams and plots from these works that illustrate some of the behavior that is typical in real reactor systems.

In particular, Figs. 11–16 (from Refs. 23 and 25) show the actual fuel assembly design, the detailed 2-D XY core configuration that was modeled, a corresponding set of typical X-directed and Y-directed flux profiles near the core centerline, and the top view of a 2-D surface plot showing the overall power density distribution within this specific 21-element core layout (note that all the control blades are in the out position in these XY models for the axial centerline of the UMLRR). From the geometry diagram, note that each assembly is broken into five regions to accommodate the specific design of the UMLRR LEU fuel assembly as shown in Fig. 11 -- where the top and bottom regions account for the non-fueled portions of the fuel plates and the side plates that hold the individual fuel plates in place, the left and right regions of the assembly model the dummy aluminum plates on both ends of the assembly, and the homogenized central region contains most of the actual fuel plates and water channels within the overall assembly.

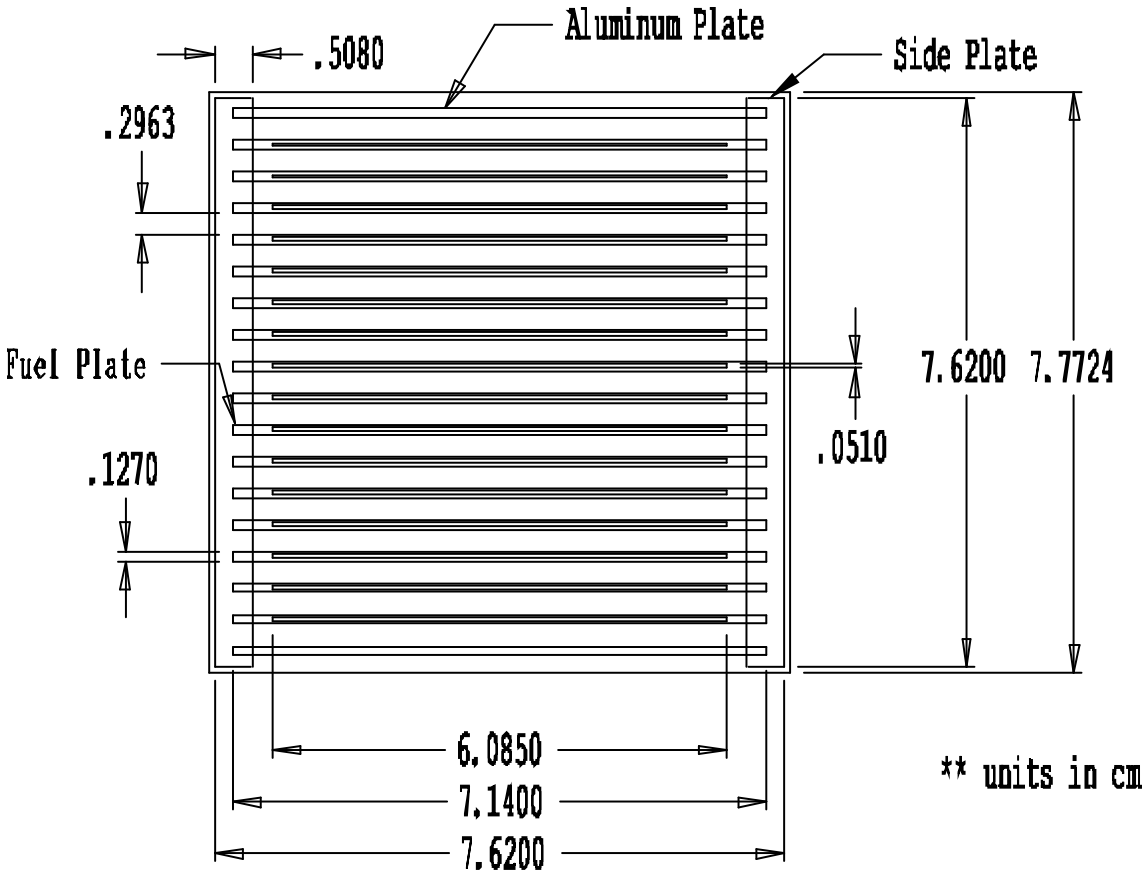

Fig. 11 Standard LEU1618 fuel assembly geometry.
(This sketch is rotated 90° relative to the assembly arrangement in the core – see Fig. 12.)

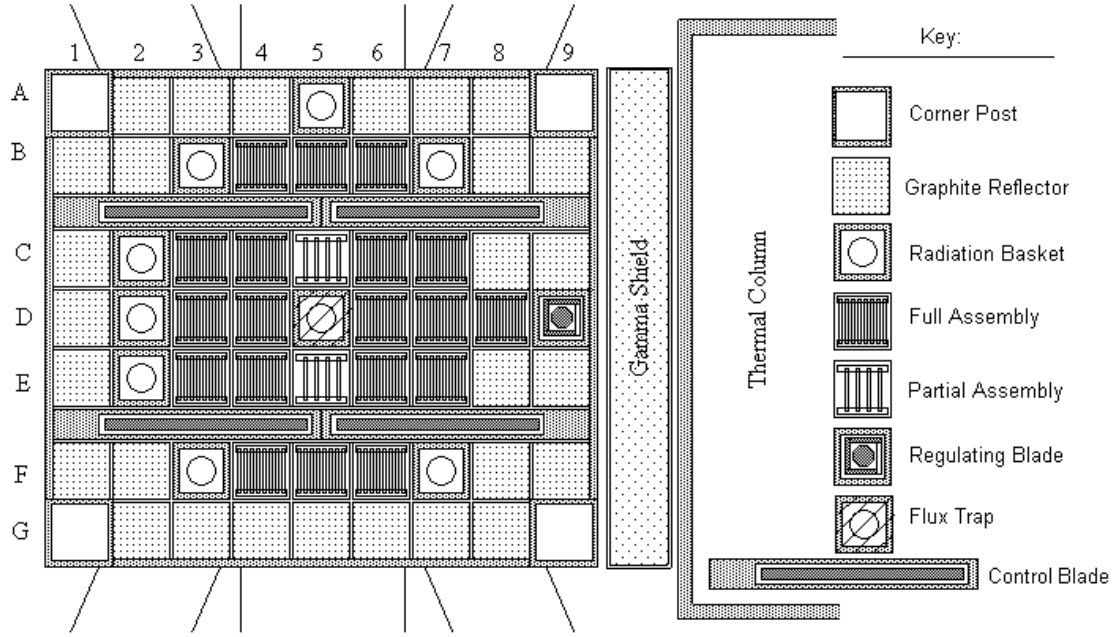

Fig. 12 Core layout for the reference LEU fuel design in the UMLRR.

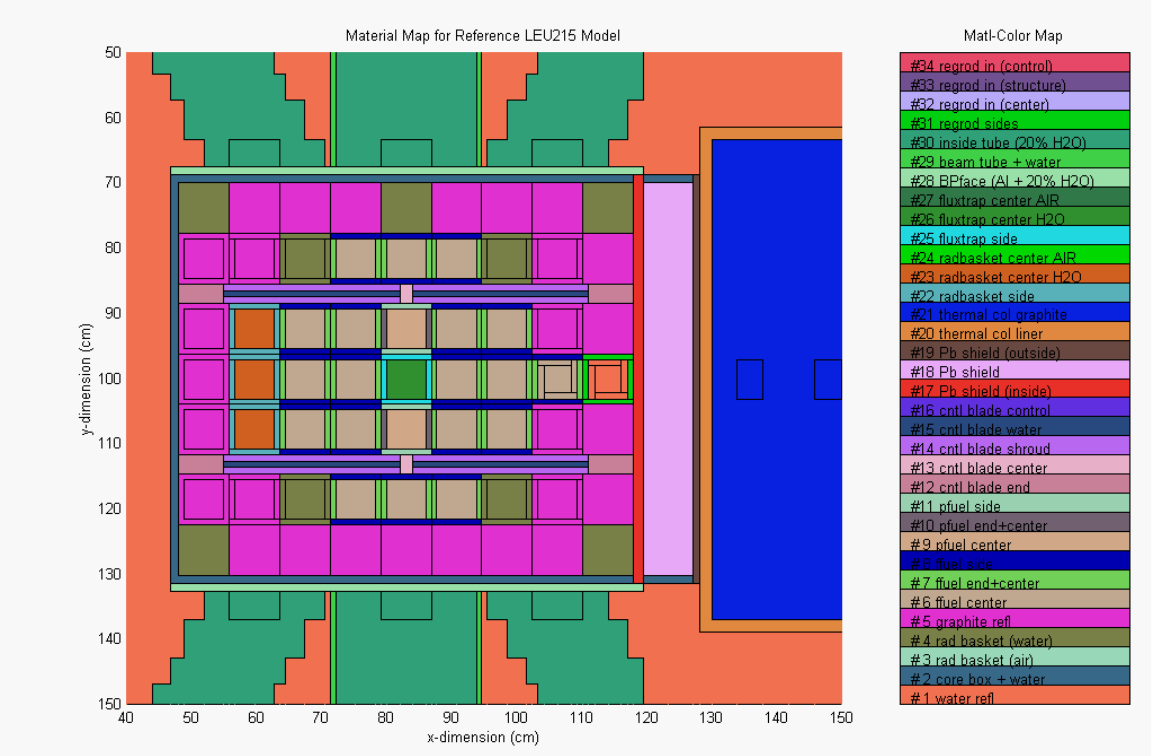

Fig. 13 Zone and material map for the reference LEU215 core.

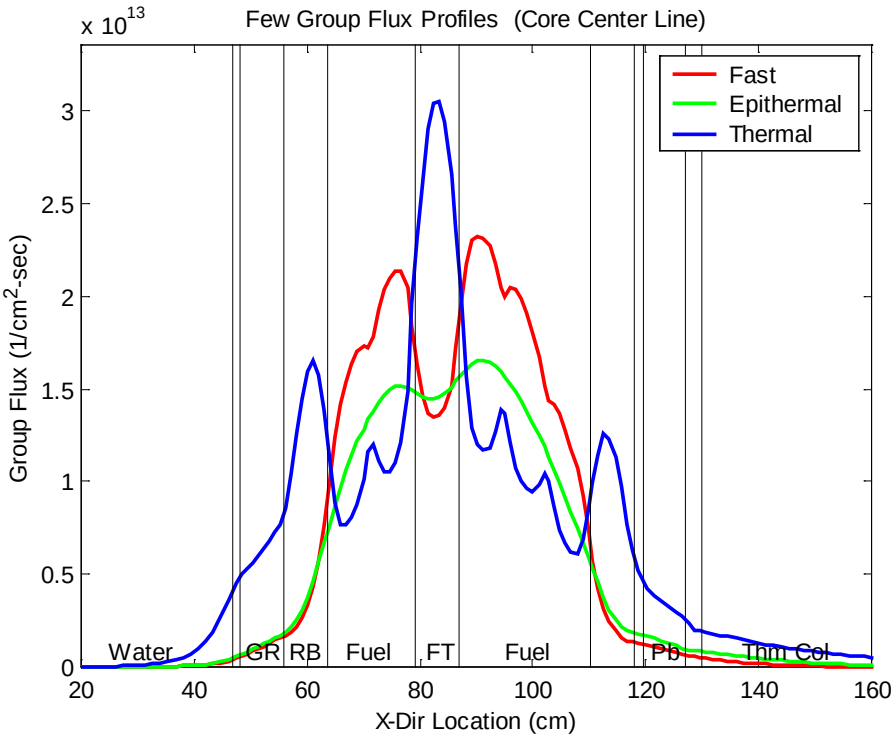

Fig. 14 Typical X-directed flux profiles along the core centerline.

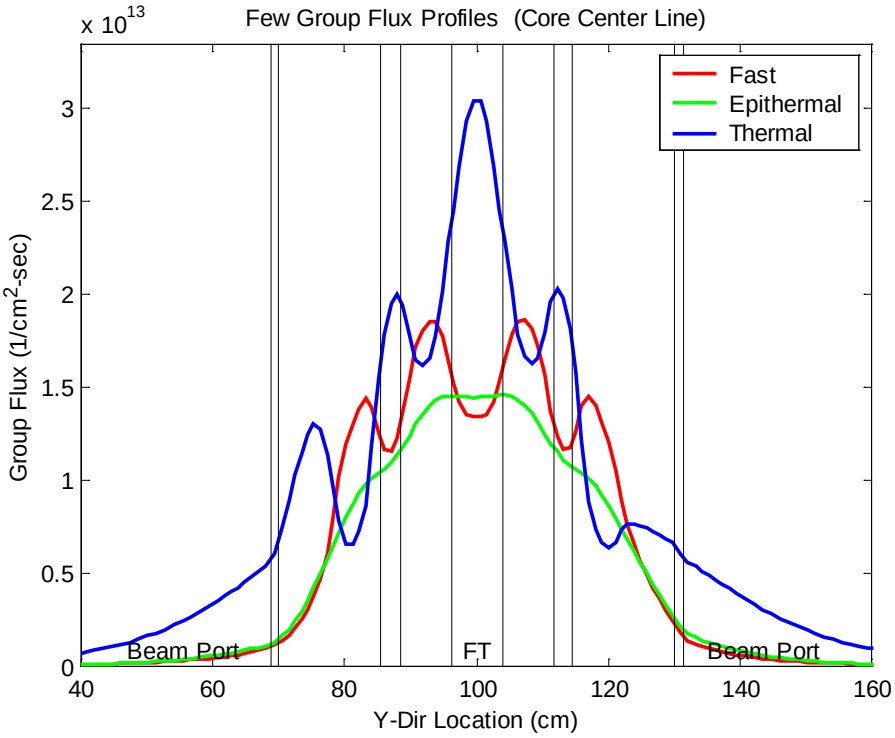

Fig. 15 Typical Y-directed flux profiles along the core centerline.

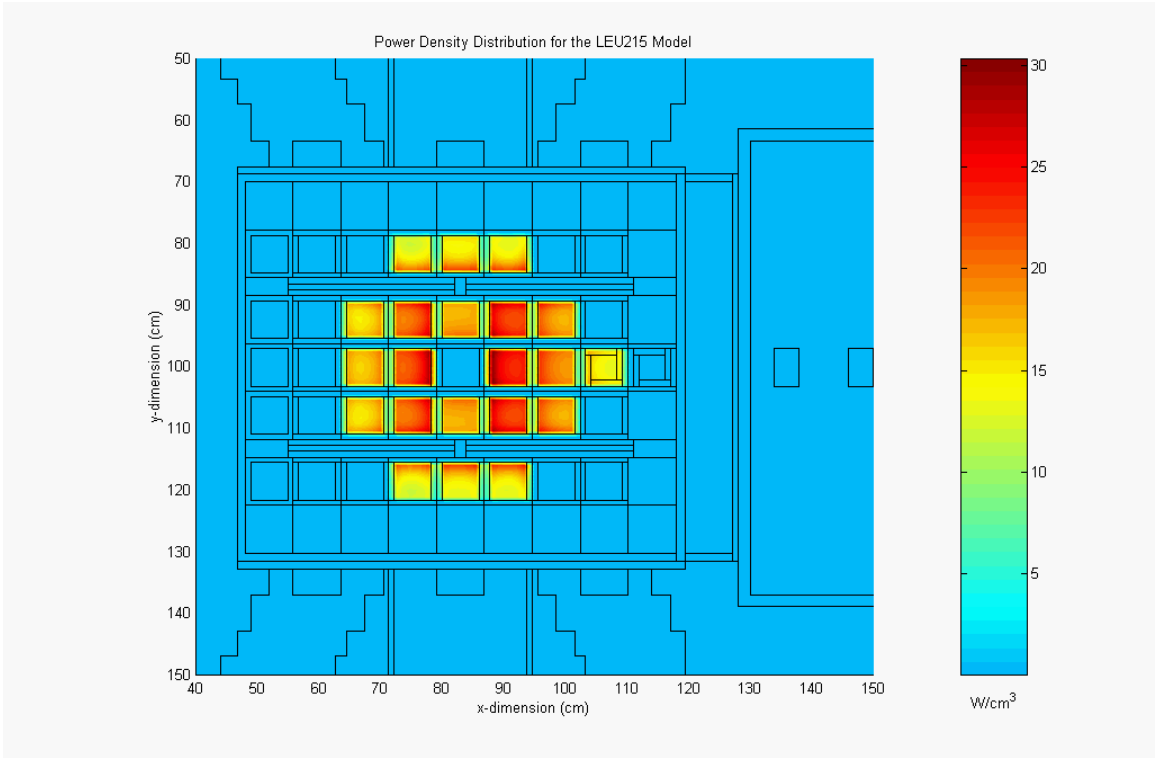

Fig. 16 2-D XY power distribution for the reference LEU215 core.

The geometry details associated with the assembly design are important, since the changes in the macroscopic cross sections between individual regions within the assembly and among the different element types (full fuel, partial fuel, water filled radiation basket, graphite reflector, etc.) give rise to much of the detailed structure seen in the flux and power density plots shown here. For example, the three large peaks in the thermal flux in the X-directed flux profiles in Fig. 14 are due to the radiation basket (RB) on the left, the central flux trap (FT) assembly, and the regulating blade region (in its control-out configuration) on the right. The smaller intermediate peaks -- one on the left of the flux trap and two on the right side of the FT assembly -- are due to the dummy aluminum plates and unheated coolant channels on each side of the fuel assembly. These water and aluminum regions act as small reflector zones where the thermal flux peaks due to the slowing down of the fast neutrons from the nearby fuel regions. Similar behavior is also apparent in the Y-directed thermal flux profile in Fig. 15, where the flux trap and the two water-filled control blade channels (remember that the control is out in this model) account for the three large flux peaks in this figure. Also notice that the localized peak on the left side (at $y \approx 75$ cm) is due to the water-filled radiation basket in this location (used as a source holder), and the smaller broader thermal flux peak on the right side of the model (at $y \approx 125$ cm) is due to the graphite reflector block in this location -- where we recall that graphite has a much larger diffusion length than water and, therefore, the reflector peaks are usually not as large in graphite relative to water.

Concerning the fast flux distributions, much of the above discussion is also appropriate if we remember that the fast neutrons are born in the fuel regions and simply slow down to thermal in the non-fuel locations. Thus, we would expect the fast flux to peak in the fuel and dip in the water and graphite non-fuel zones -- and careful inspection of the flux profiles in Figs 14 and 15 and the geometry layout in Fig. 13 shows that the calculated fast flux behavior is exactly as expected.

Finally, we note that the power density distribution shown in Fig. 16 is also as expected. Here, of course, power is only produced in the fueled regions (we assume that the power is deposited at the location of the fission event) and, since most of the fissions are at thermal energies, the power density follows the thermal flux distributions in the fuel fairly closely. Thus, we see that the power density peaks occur on the edges of the fuel assemblies (and not in the center of the elements) because of the thermal flux peaks in the neighboring water regions. From Fig. 16 we see that the peak power density is about 30 W/cm^3 and that this occurs in the fuel assembly just to the right of the central flux trap element -- in fact, to reduce this peak power density somewhat, the flux trap has a central region of water (or the experimental basket) and an outer graphite rim, since the use of graphite versus water tended to reduce the peak power density somewhat without a significant penalty in the experimental thermal flux that could be achieved.

The results for the LEU215 core model as described above were obtained during the design phase of the HEU to LEU conversion effort -- these represented the predicted behavior of the new LEU core. Once the new core was actually installed, startup physics testing showed that the initial core excess reactivity was slightly lower than predicted. Thus, a small change was made that interchanged four water reflectors assemblies with four graphite reflectors to give a small increase in reactivity -- as shown in Fig. 17. The new model was referred to as the LEU216/LEU316 model for computational purposes and this became the actual initial LEU core configuration for the UMLRR (denoted as the M-1-3 core by the operations staff).

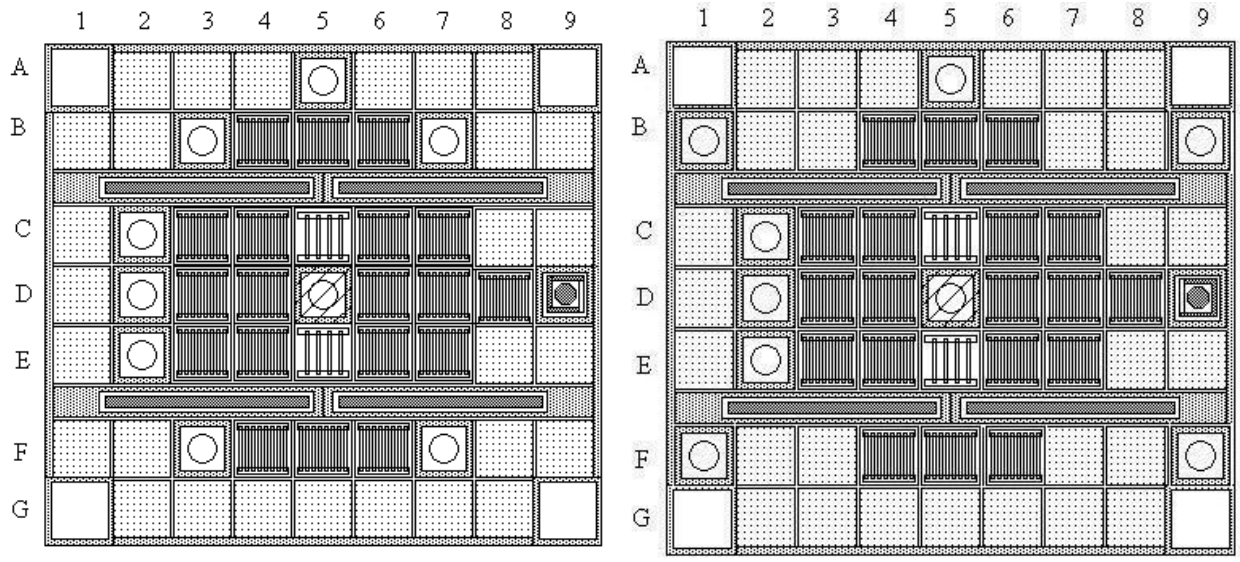

Fig. 17 Target (left) and actual (right) startup cores for the LEU-fueled UMLRR.

Five copper wires (and two gold normalization foils) were inserted in the M-1-3 official startup core in the locations shown in Fig. 18, and these were irradiated to produce radioactive Cu-64. After irradiation, the wires were cut into 1-inch segments and, from the measured activity of each of the wire segments, one can deduce the axial profile of the thermal flux in the particular XY grid location. Figure 19 shows the resultant measured and calculated axial profiles for the UMLRR. Although there are some noticeable differences, the axial profiles are represented reasonably well by the VENTURE calculations -- these flux comparisons and several additional measured reactivity worths and the measured differential worth curves for the five control elements within the UMLRR gave good confidence in the overall performance of the VENTURE modeling.[19]

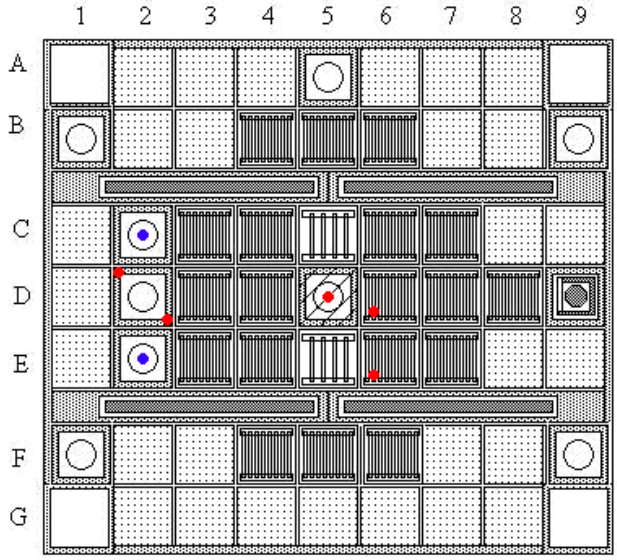

Fig. 18 Location of the gold foils and copper wires for the flux mapping measurements.

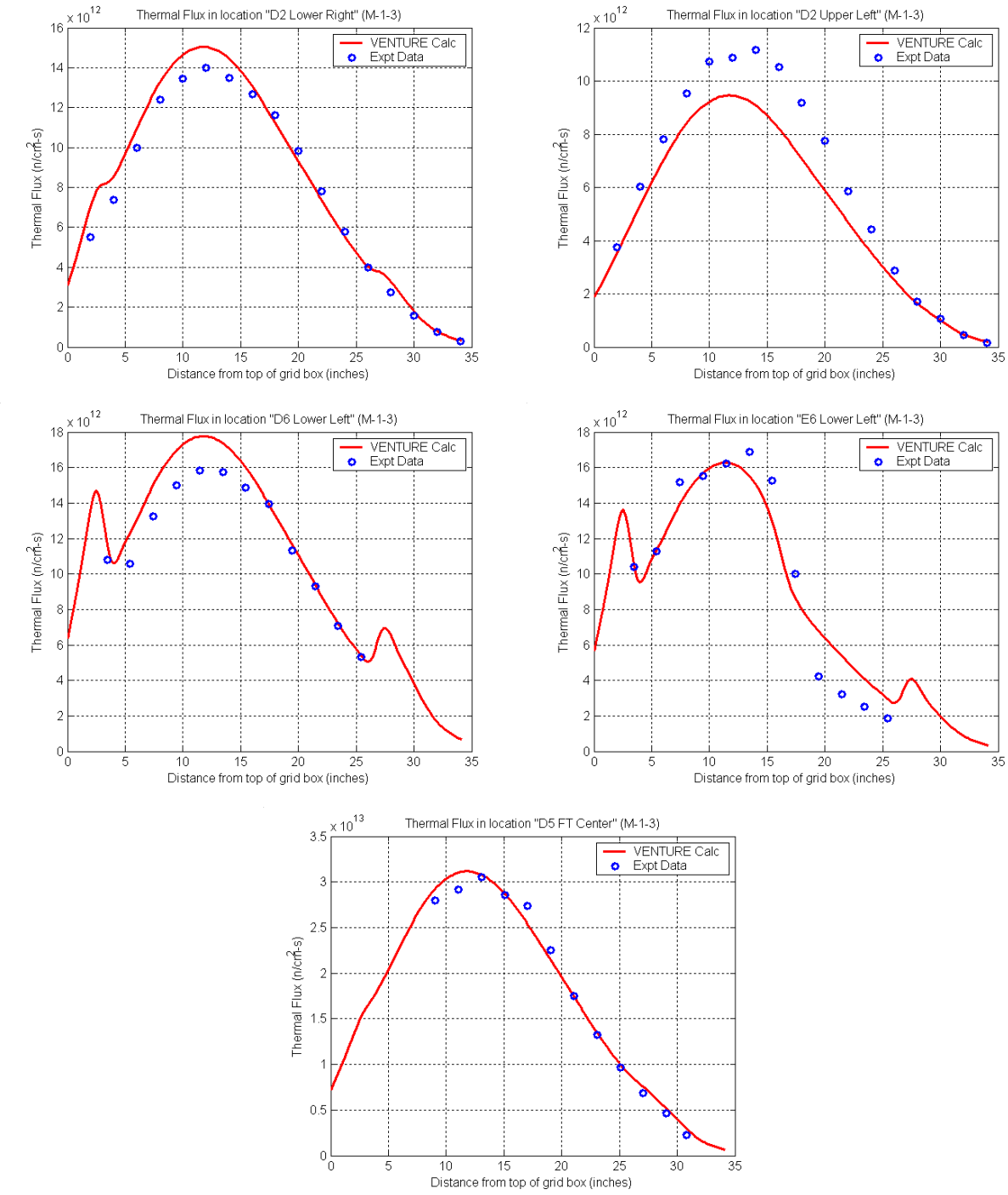

Fig. 19 Measured and computed axial thermal flux profiles at various locations (M-1-3).

As a final modeling example, a series of pictures, diagrams, and modeling results associated with the design and analysis of the fast neutron irradiator (FNI) within the UMLRR are summarized below (from Refs. 20 and 21). The purpose of this new experimental facility was to provide an easily accessible large-volume irradiation facility that had a relatively uniform fast flux $\geq 10^{11}$ n/cm^2-s over a 1 ft^2 area parallel to the side of the core, that minimized the thermal neutron fluence rate and gamma dose to the extent possible, and that had a maximum reactivity effect below the limit for movable experiments within the UMLRR (so that samples could be inserted and/or removed during full power operation). To achieve these goals, three existing beam ports were removed from one side of the core and a modular arrangement consisting of a large volume sample canister, several shield blocks, a large aluminum guide collar, four aluminum blocks, and a single flux shaping element was constructed within an aluminum grid support structure similar to the core grid structure (as shown in the pictures given below in Figs. 20-23).

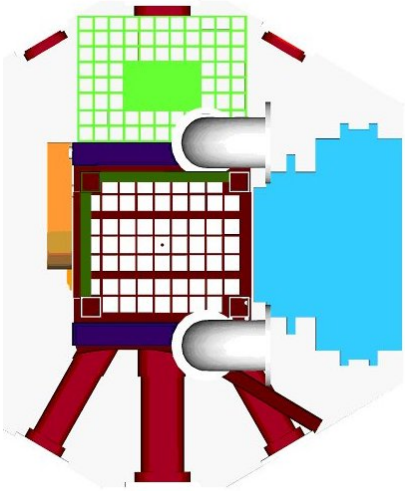

Fig. 20 Side view of FNI during installation.

Fig. 21 Top view of FNI during installation.

Fig. 22 FNI configuration with Al collar.

Fig. 23 Photo of large sample canister.

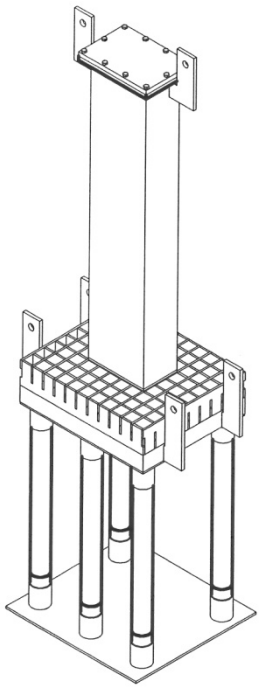

Two-dimensional computational models in both XY and YZ orientations were generated to assist in the design and analysis of the new FNI facility, where Figs. 24 and 25 show the zone and material layouts for the final version of these models. As apparent, a number of changes to the core region were needed to accommodate the new experimental facility (new arrangement of fuel assemblies, movement of the startup source, addition of five leaded void boxes, etc.) and a whole new experimental facility replaced the three beams ports on one side of the core.

Although there were a significant number of calculations and intermediate results generated during the whole development effort, only a few of the final summary results are given here (see Refs. 20 and 21 for further details). In particular, Fig. 26 shows the overall effectiveness of the basic FNI design (with lots of borated aluminum and lead in the FNI shield blocks) in attenuating the low energy and gamma fluxes to a greater extent relative to the fast flux component -- with a fast flux in the experimental region that slightly exceeds the design specification of 10^{11} n/cm^2-s. This is also summarized in Table 3, where we see several integral indicators that compare an in-core radiation basket facility with the ex-core FNI facility. Finally, Fig. 27 shows the absolute and normalized neutron spectra in the in-core D2 and ex-core FNI sample locations. Certainly the ex-core facility has a lower thermal flux component but, as apparent, this benefit was obtained at the expense of a reduced fast flux level. In addition, as illustrated in the normalized plot of just the fast spectra (Fig. 27b), the high energy end of the energy profile is also degraded somewhat -- and this is the inevitable, but undesirable result of having an easily accessible ex-core irradiator (since there will always be some moderation of the high energy neutrons when passing through any medium -- even high mass number materials). Overall, however, the fast-to-thermal and fast-to-gamma flux ratios in the FNI are much greater than in the in-core irradiation location -- thus, the new facility does indeed meet its intended role as an accessible large-volume fast neutron irradiator.

Summary

Well, we have finally completed this section of Lecture Notes. We started this lesson with a base understanding of multigroup diffusion theory, but we had no practical knowledge of the application of that theory to real design and analysis situations. Now, upon completion of this section of the course, you have been exposed to a variety of applications, ranging from simple 1-group source-driven and critical systems to the detailed design and analysis of a new LEU fueled core and a new ex-core experimental facility for the UMLRR. Along the way, a number of useful analytical procedures were developed for performing preliminary critical size and critical composition calculations, for determining the flux profile and magnitude in a number of simple configurations, for computing peaking factors, fast-to-thermal flux ratios, etc., for addressing the elements of the four and six factor formulas and relating these to the general life-cycle of a neutron in thermal systems, for addressing heterogeneous effects, and for extending and applying the concepts treated in our simple analytical treatments to the design and analysis of realistic systems. In all, we have done a lot here, and a good understanding of this material will help give you a strong foundation for future studies and/or work within the reactor physics area!

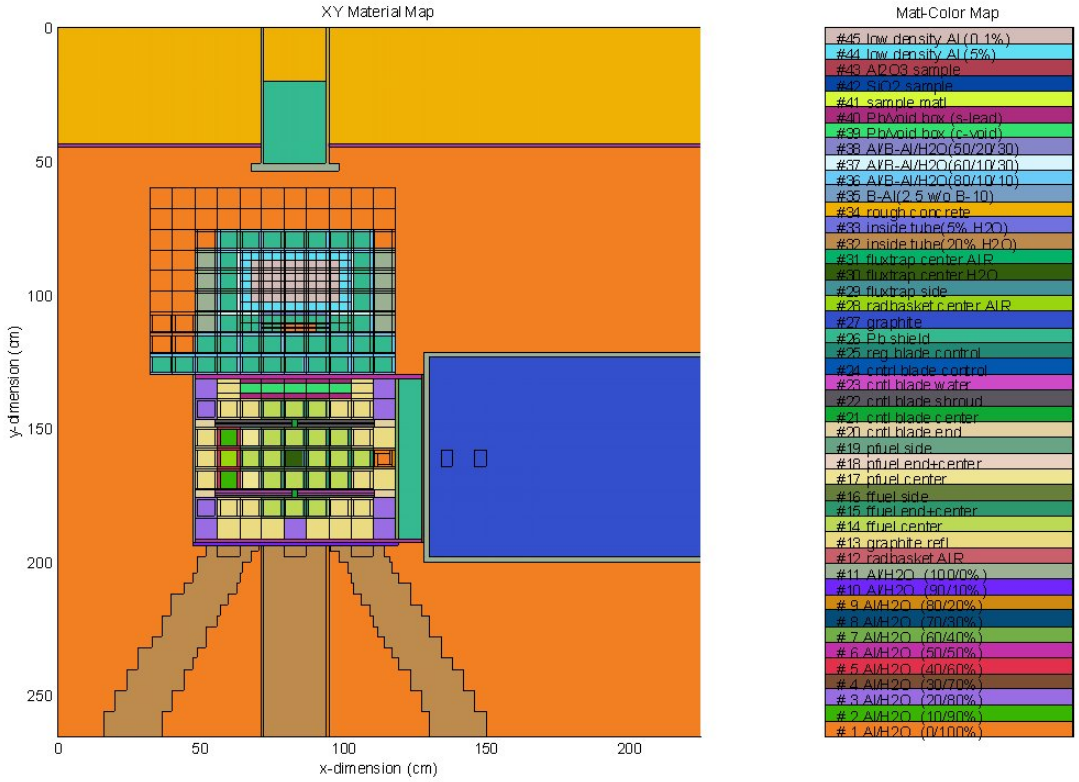

Fig. 24a Full view of XY computational model.

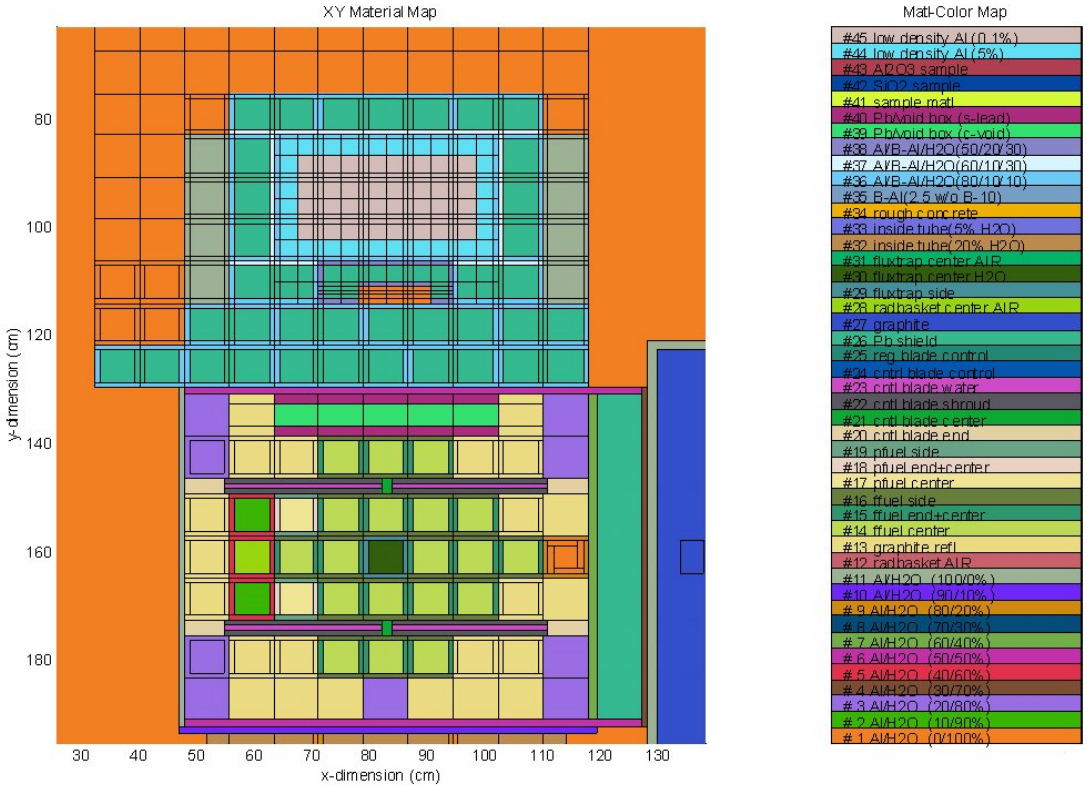

Fig. 24b Expanded view of core and FNI from XY computational model.

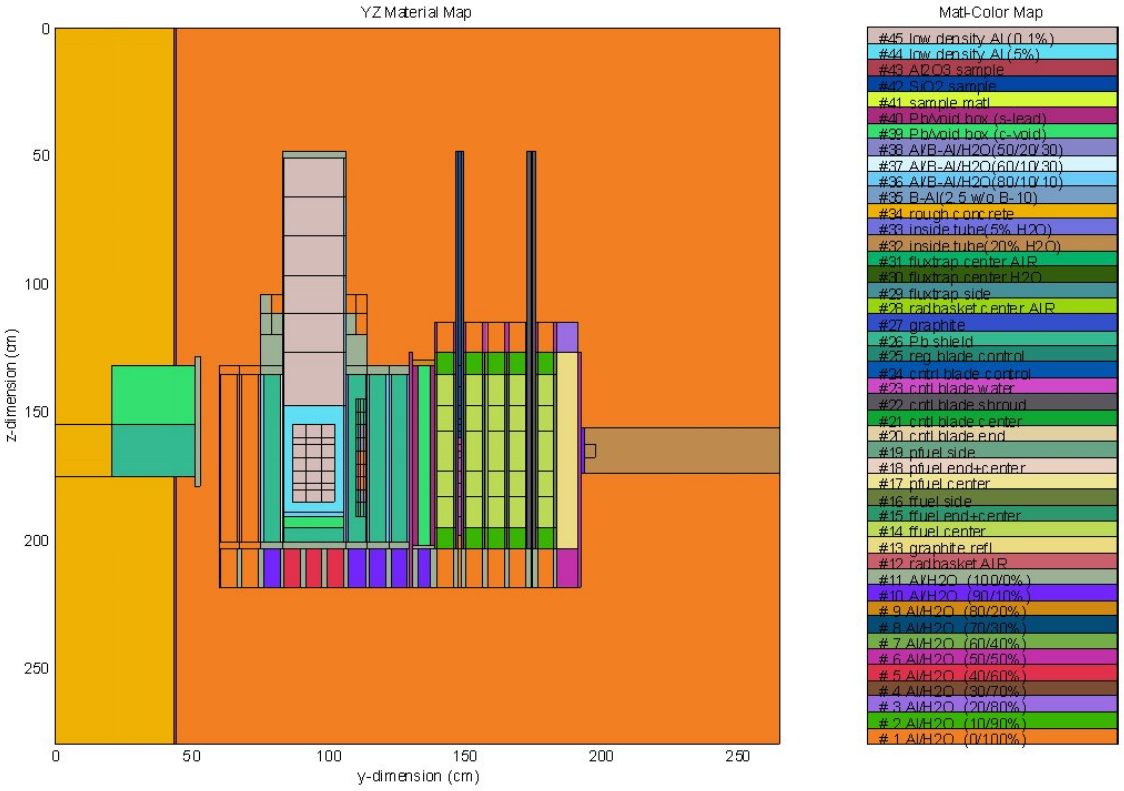

Fig. 25a Full view of YZ computational model.

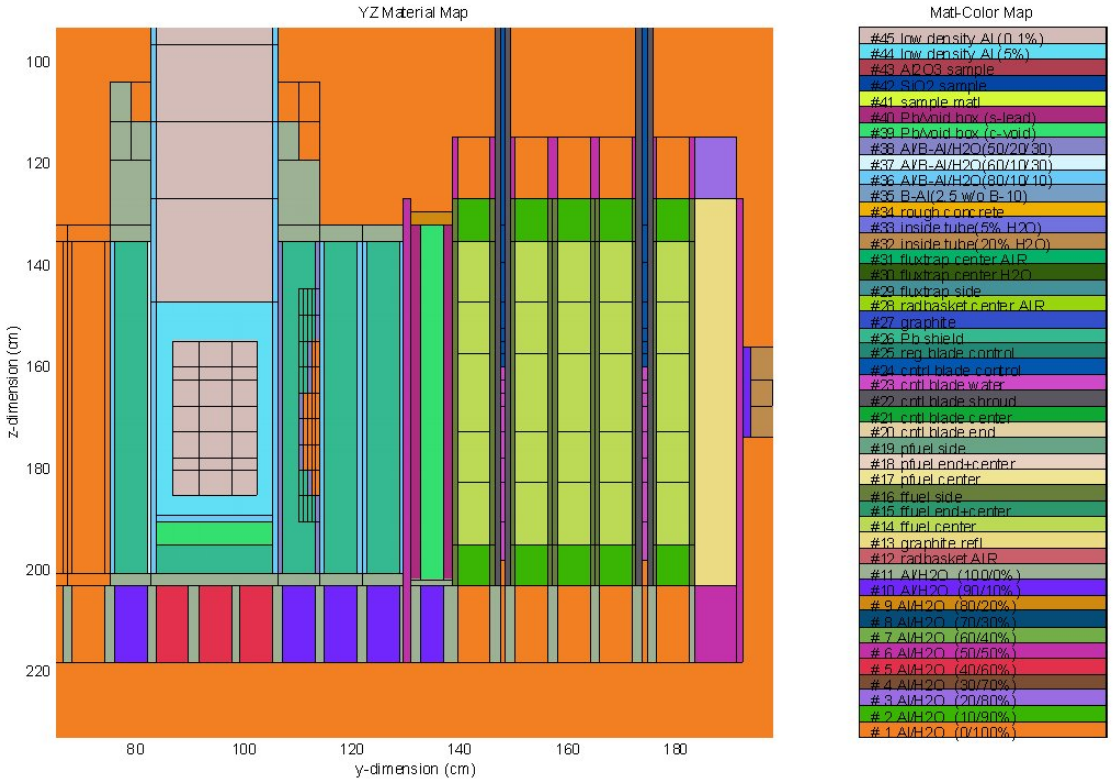

Fig. 25b Expanded view of core and FNI from YZ computational model.

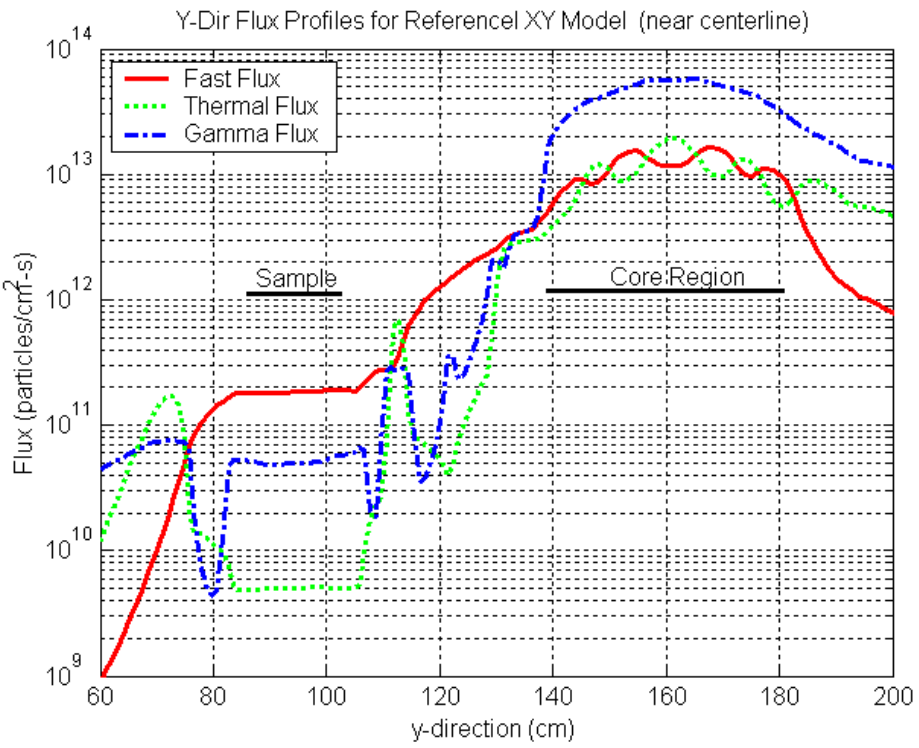

Fig. 26 Y-directed flux profiles from the DORT XY model.

Table 3 Integral parameters for in-core location D2 and the new ex-core FNI facility.

Parameter of Interest	Radiation Basket D2	FNI Sample
Broad Group Fluxes (n/cm^2-sec)		
Fast Flux > 0.1 MeV	3.26E+12	1.83E+11
Epithermal Flux	3.42E+12	2.45E+11
Thermal Flux < 1 eV	1.14E+13	4.85E+09
Total Neutron Flux	1.81E+13	4.33E+11
Total Gamma Flux	2.95E+13	5.05E+10
Additional Fast Flux Characterization		
Fast Flux > 1 MeV	1.72E+12	5.08E+10
Fast Flux > 0.01 MeV	4.02E+12	2.55E+11
1 MeV Equiv. Flux	3.08E+12	1.39E+11
RDF	0.77	0.55
Energy Deposition Rates (Krad/hr)		
Neutrons in Air	2.58E+04	1.38E+02
Neutrons in Silicon	9.37E+02	3.20E+01
Gammas in Air	3.50E+04	4.40E+01
Gammas in Silicon	3.74E+04	4.62E+01

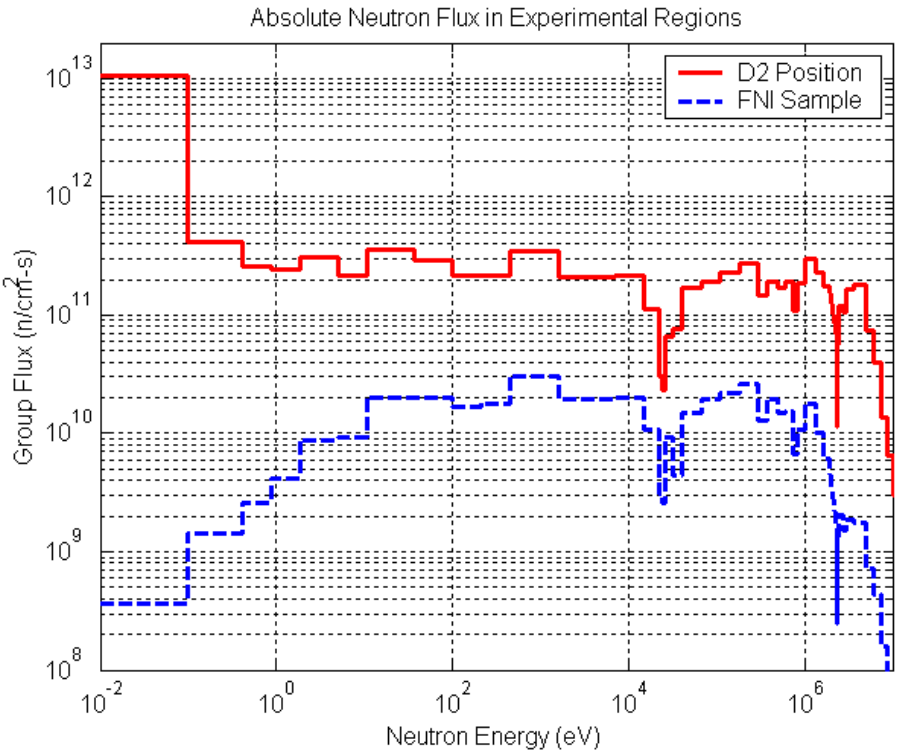

Fig. 27a Absolute neutron flux in two experimental facilities within the UMLRR.

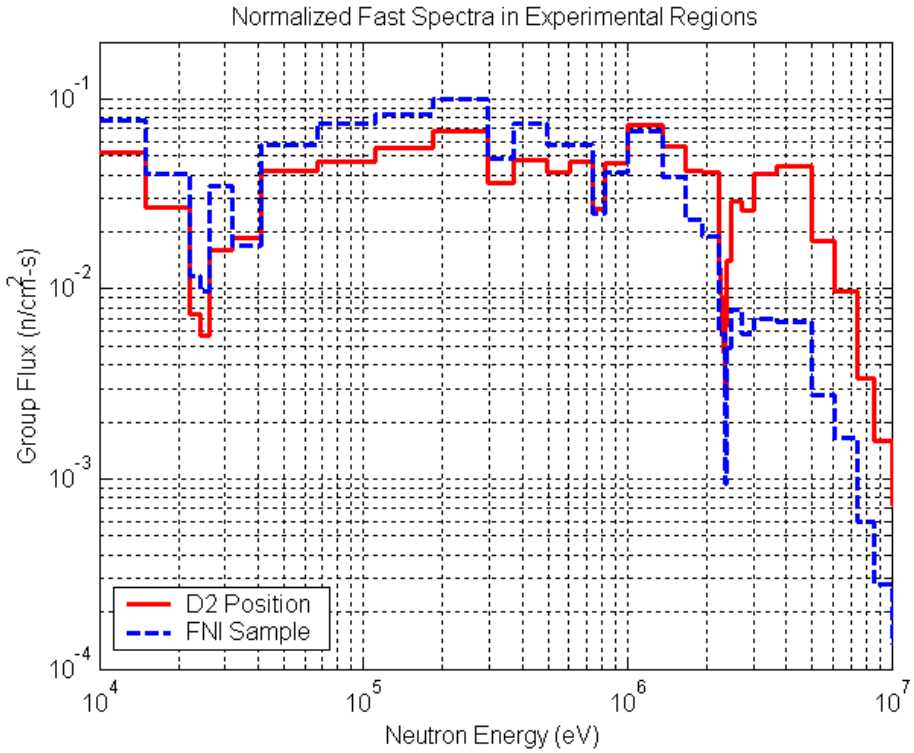

Fig. 27b Normalized fast neutron spectra within the D2 and FNI regions.

References

1. J. R. White, "The Multigroup Neutron Balance Equation," part of a series of Lecture Notes for the Nuclear Engineering Program at UMass-Lowell.
2. J. R. Lamarsh and A. J. Baratta, ***Introduction to Nuclear Engineering***, 3rd Edition, Prentice Hall (2001).
3. J. R. White, "Planar Source in a Moderating Medium," part of a series of Lecture Notes for the Nuclear Engineering Program at UMass-Lowell. This set of Lecture Notes also provides documentation for the ***slabmm_gui*** Matlab program.
4. J. R. White, "Point Source in a Moderating Medium," part of a series of Lecture Notes for the Nuclear Engineering Program at UMass-Lowell. This set of Lecture Notes also provides documentation for the ***spheremm_gui*** Matlab program.
5. J. R. White, "Two-Region Slab with a Planar Source at the Interface," part of a series of Lecture Notes for the Nuclear Engineering Program at UMass-Lowell. This set of Lecture Notes also provides documentation for the ***two-regions_gui*** Matlab program.
6. J. R. White, "Two Planar Sources in an Infinite Moderating Medium," part of a series of Lecture Notes for the Nuclear Engineering Program at UMass-Lowell. This set of Lecture Notes also provides documentation for the ***two_planar_sources_gui*** Matlab program.
7. J. R. White, "Interpretation of the Diffusion Length," part of a series of Lecture Notes for the Nuclear Engineering Program at UMass-Lowell.
8. J. R. White, "Cross Section Data for Preliminary Calculations," part of a series of Lecture Notes for the Nuclear Engineering Program at UMass-Lowell. This set of Lecture Notes also provides documentation for the ***cross_sections_gui*** Matlab program.
9. J. R. White, "A 2-Group Example: Point Source of Fast Neutrons in an Infinite Moderating Medium," part of a series of Lecture Notes for the Nuclear Engineering Program at UMass-Lowell.
10. J. R. White, "1-D Bare and Reflected Critical Systems Using 1-Group Diffusion Theory," part of a series of Lecture Notes for the Nuclear Engineering Program at UMass-Lowell. This set of Lecture Notes also provides documentation for the ***core_refl1g_gui*** Matlab program.
11. J. R. White, "Overview of Bessel Functions," part of a series of Lecture Notes for the Nuclear Engineering Program at UMass-Lowell.
12. J. R. White, "The Bare Critical Finite Cylindrical Reactor," part of a series of Lecture Notes for the Nuclear Engineering Program at UMass-Lowell.
13. J. R. White, "2-Group Diffusion Theory for Critical Systems," part of a series of Lecture Notes for the Nuclear Engineering Program at UMass-Lowell. This set of Lecture Notes also provides documentation for the ***diluteh_gui*** Matlab program.
14. J. R. White, "Neutron Interactions with Matter," part of a series of Lecture Notes for the Nuclear Engineering Program at UMass-Lowell.
15. "VENTURE-PC - A Reactor Analysis Code System," Radiation Safety Information Computational Center, CCC-654 (1997).

16. Benchmark Problem Book, ANL-7416, Suppl. 2, Argonne National Laboratory (1977). The actual figure used here was obtained from the following website: https://engineering.purdue.edu/PARCS/Code/TestSuite/CalculationMode/StandAloneMode/Eigenvalue/IAEA3DPWR

17. "DOORS3.1 - One, Two, and Three Dimensional Discrete Ordinates Neutron/Photon Transport Code System," Radiation Safety Information Computational Center, CCC-650 (1996). The 2-D DORT code is part of the DOORS computational system.

18. J. R. White and L. M. Bobek, "HEU to LEU Conversion Experience at the UMass-Lowell Research Reactor," 9th International Topical Meeting on Research Reactor Fuel Management, Budapest, Hungary (April 2005).

19. J. R. White and L. Bobek, "Startup Test Results and Model Evaluation for the HEU to LEU Conversion of the UMass-Lowell Research Reactor," 24th Intl. Mtg. on Reduced Enrichment for Research and Test Reactors, San Carlos de Bariloche, Argentina (Nov. 2002).

20. J. R. White, L. M. Bobek, and T. M. Regan, "Initial Testing of the New Ex-Core Fast Neutron Irradiator at the UMass-Lowell Research Reactor," UMass-Lowell Informal Project Documentation (June 2002).

21. J. R. White, A. Jirapongmed, L. Bobek, and T. M. Regan, "Design and Initial Testing of an Ex-Core Fast Neutron Irradiator for the UMass-Lowell Research Reactor," 2002 ANS Radiation Protection and Shielding Topical Conference, Santa Fe, NM (April 2002).

22. J. R. White, J. Byard, and A. Jirapongmed, "Calculational Support for the Startup of the LEU-Fueled UMass-Lowell Research Reactor," Proceedings of Topical Meeting on Advances in Reactor Physics and Mathematics and Computation, Pittsburgh, PA (May 2000).

23. J. R. White, A. Jirapongmed, and J. Byard, "Preliminary Characterization of the Irradiation Facilities Within the LEU-Fueled UMass-Lowell Research Reactor," Proceedings of Topical Meeting on Advances in Reactor Physics and Mathematics and Computation, Pittsburgh, PA (May 2000).

24. J. R. White and R. D. Tooker, "Modeling and Reference Core Calculations for the LEU-Fueled UMass-Lowell Research Reactor," ANS 1999 Winter Meeting, Long Beach, CA (Nov. 1999).

25. J. R. White, "Cross Section Libraries and Preliminary Modeling for the Reference UMLRR LEU Core Configuration," UMass-Lowell Informal Project Documentation (Jan. 1999).